Check for updates

Received: 11 April 2023 | Revised: 16 August 2023 | Accepted: 15 September 2023

DOI: 10.1111/1541-4337.13250

COMPREHENSIVE REVIEW

Comprehensive REVIEWS in Food Science and Food Safety WILEY

A review on plasma-activated water and its application in the meat industry

Koentadi Hadinoto[1] | **Brendan A. Niemira**[2] | **Francisco J. Trujillo**[1]

[1]School of Chemical Engineering, University of New South Wales, Sydney, New South Wales, Australia

[2]USDA-ARS, Eastern Regional Research Center, Food Safety and Intervention Technologies Unit, Wyndmoor, Pennsylvania, USA

Correspondence
Francisco J. Trujillo, School of Chemical Engineering, University of New South Wales, Sydney, New South Wales, Australia. Email: francisco.trujillo@unsw.edu.au

Abstract

Meat is a nutritious food with a short shelf life, making it challenging to ensure safety, quality, and nutritional value. Foodborne pathogens and oxidation are the main concerns that lead to health risks and economic losses. Conventional approaches like hot water, steam pasteurization, and chemical washes for meat decontamination improve safety but cause nutritional and quality issues. Plasma-activated water (PAW) is a potential alternative to thermal treatment that can reduce oxidation and microbial growth, an essential factor in ensuring safety, quality, and nutritional value. This review explores the different types of PAW and their physiochemical properties. It also outlines the reaction pathways involved in the generation of short-lived and long-lived reactive nitrogen and oxygen species (RONS) in PAW, which contribute to its antimicrobial abilities. The review also highlights current studies on PAW inactivation against various planktonic bacteria, as well as critical processing parameters that can improve PAW inactivation efficacy. Promising applications of PAW for meat curing, thawing, and decontamination are discussed, with emphasis on the need to understand how RONS in PAW affect meat quality. Recent reports on combining PAW with ultrasound, mild heating, and non-thermal plasma to improve inactivation efficacy are also presented. Finally, the need to develop energy-efficient systems for the production and scalability of PAW is discussed for its use as a potential meat disinfectant without compromising meat quality.

KEYWORDS

food safety, meat safety, non-thermal plasma, non-thermal processing, plasma-activated water

1 | INTRODUCTION

Meat is highly regarded as a nutritious food due to its abundance of essential nutrients such as protein, iron, vitamin B12, other B complex vitamins, zinc, selenium, and phosphorus (Pereira & Vicente, 2013). The global demand for meat continues to rise due to economic growth and increasing populations (Giller et al., 2021). Despite the high nutritional value of meat, it remains a delicate product with a short shelf life. This presents a significant challenge in ensuring the safety, quality, and nutritional value of meat products. Foodborne pathogens pose a significant

This is an open access article under the terms of the Creative Commons Attribution-NonCommercial-NoDerivs License, which permits use and distribution in any medium, provided the original work is properly cited, the use is non-commercial and no modifications or adaptations are made.
© 2023 The Authors. *Comprehensive Reviews in Food Science and Food Safety* published by Wiley Periodicals LLC on behalf of Institute of Food Technologists.

risk to consumers, causing over five million cases of foodborne illnesses in Australia annually (Kirk et al., 2014). Controlling microbial growth and contamination in fresh meat is challenging because of the complexity of the meat matrix, making it an excellent substrate for the growth of microorganisms. The growth of microorganisms such as *Campylobacter*, *Escherichia coli*, *Listeria*, *Salmonella*, and *Staphylococcus aureus*, can lead to food waste and economic losses while posing health risks to consumers (Kim et al., 2021; Nastasijević et al., 2017). Therefore, the elimination of foodborne pathogens from farm to table is crucial.

In addition to microbial growth, meat is susceptible to oxidation, which is the main non-microbial source of quality degradation in meat and meat products. Oxidation leads to the loss of essential fatty acids and vitamins and causes rancidity, and changes in meat odor, flavor, and color (Dominguez et al., 2019). These undesirable changes affect consumer acceptance, and lipid oxidation decreases the shelf life of meat because of the production of toxic substances such as aldehydes, ketones, and hexanes (Kalogianni et al., 2020). As such, the meat industry is in search of effective approaches to limit the extent of lipid oxidation. Hence, addressing the challenges of microbial growth and oxidation in meat products is vital to ensure the safety, quality, and nutritional value of meat products while meeting the increasing global demand.

For decades, hot water, steam pasteurization, and chemical washes have been used to eliminate foodborne pathogens, improving meat safety but causing nutritional and quality problems of treated meat and meat products (Roobab et al., 2022; Rosario et al., 2021). Chemical residues on the meat surfaces may result in health complications for consumers (Roobab et al., 2022). Chlorine, for instance, may interact with organic compounds, creating carcinogenic trihalomethanes (Han et al., 2021).

Beyond these methods, many researchers have studied non-thermal plasma (NTP) as a potential solution to substitute thermal treatments in food decontamination and to increase shelf life (Chiozzi et al., 2022; Degala et al., 2018). Plasma is the fourth state of matter, besides solid, liquid, and gas, owing to an increase in the energy of gases that results in the ionization of some of the atoms and molecules in gases (Bai et al., 2020; Rivero et al., 2022). Plasma can be regarded as an ionized gas that is rich in ions, electrons, free radical species, uncharged particles, quanta of electromagnetic radiation, and strong electric fields, making the plasma highly electrically conductive (Bai et al., 2020). In general, there are two types of plasma, thermal plasma, which is produced with temperatures ranging from 6000 to 20000 K (Tabu e, 2022), and NTP.

NTP, also known as cold plasma, is a partially ionized gas with a temperature close to room temperature (25 to 100°C) (Simoncicova et al., 2019; Tabares & Junkar, 2021). It can be generated under atmospheric conditions with electromagnetic sources and configurations such as pin-to-liquid discharge, glow discharge, dielectric barrier discharge (DBD), and plasma jet (Ghimire et al., 2021; Lu et al., 2017; Neretti et al., 2016; Yoon et al., 2018). Recently, NTP has gained interest for bacteria inactivation, fungal inactivation, food application, surface treatment, water treatment, agriculture, and biomedical purposes (Balan et al., 2018; Kaushik et al., 2018; Lin et al., 2023; Simoncicova et al., 2019). Depending on the application of NTP, its efficacy is affected by several parameters, such as input power, voltage, frequency, treatment time, and gas composition (Mir et al., 2020).

Although NTP possesses effective microbial decontamination of food products, this chemical-free technology still faces challenges, including developing adverse color changes, reductions in the sensory and texture quality of foods, and showing difficulties to treat large surface areas and volumes of food products, especially for foods with surface textures that are not uniform. The free radical species in NTP oxidize meat products that are high in lipids, causing rancidity and contributing to spoilage (Jadhav & Annapure, 2021). To overcome these challenges, plasma-activated water (PAW) has been proposed as a solution.

Evidence suggests that PAW has the potential to be an environmental-friendly and cost-effective sanitizing process, the central aspect of which is the interaction of NTP with water to create a cocktail of highly reactive oxygen and nitrogen species (RONS), such as nitric oxide, nitrite, nitrate, and hydrogen peroxide (Liao et al., 2020; Qian et al., 2021). These species are responsible for the antimicrobial activity of PAW, inducing high oxidative stresses on bacteria and other pathogens (Liao et al., 2020).

This review describes the common generation methods of PAW and its chemistry, which govern the composition of RONS in PAW and the bactericidal efficacy of PAW for meat decontamination and provides the inactivation mechanism of PAW and processing factors influencing its inactivation efficacy. The aim is to highlight the application of PAW on meats, including fish, chicken, and beef, and the subsequent effects on meat quality and point out the gaps in PAW research related to meat.

2 | GENERATION OF PAW

The generation of PAW is broadly categorized into three modes based on the interactions between NTP and water, including plasma discharge over the water surface, direct plasma discharge in water (or underwater discharge), and multiphase plasma discharge, which have been extensively

15414337, 0, Downloaded from https://ift.onlinelibrary.wiley.com/doi/10.1111/1541-4337.13250 by CochraneArgentina, Wiley Online Library on [13/10/2023]. See the Terms and Conditions (https://onlinelibrary.wiley.com/terms-and-conditions) on Wiley Online Library for rules of use; OA articles are governed by the applicable Creative Commons License

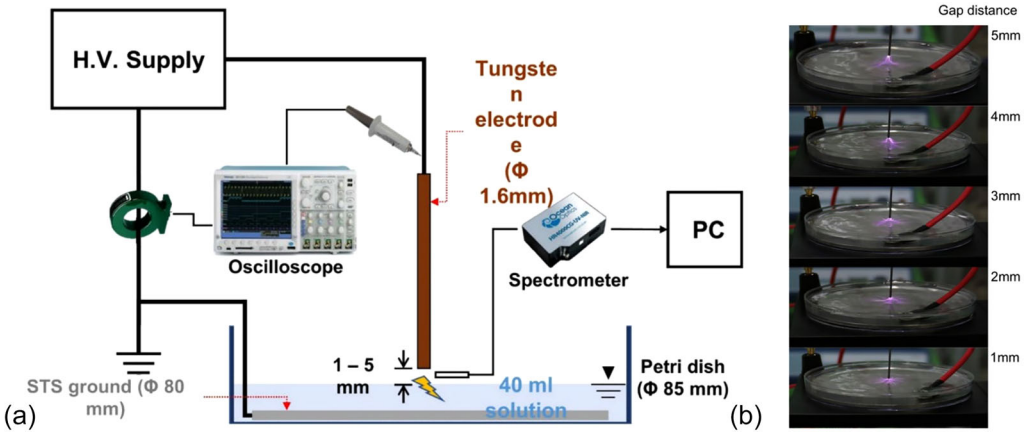

FIGURE 1 (a) Schematic diagram of the plasma device to produce plasma-activated water via a pin-to-liquid discharge and (b) images of pin-to-liquid discharge. Reproduced from Lim et al. (2022) with the permission of MDPI.

studied for applications such as antimicrobial properties, cancer treatment, enhancement of seed germination, surface treatment, and water treatment (Akiyama & Akiyama, 2020; Mai-Prochnow et al., 2021). These discharge modes along with plasma source, electron configuration, discharge gap, discharge power, and activation time not only influence the reactivity transfer from the plasma to the liquid but also affect the final composition of PAW (Subramanian et al., 2021).

Recently, multiphase plasma discharge via plasma bubbles has attracted many researchers because of its unique advantages in improving the rates of chemical reactions and the mass transfer of gaseous plasma-induced reactive species entering into the water, facilitating large volume plasma in water, and its excellent energy efficiency. Hence, this enhances the performance of plasma reactors in bacterial inactivation, algae treatment, and pollutant degradation (Hong et al., 2021; Mai-Prochnow et al., 2021; Rao et al., 2023; Sommers & Foster, 2014; Zhou et al., 2021).

Another form of multiphase plasma discharge is the discharge contacting liquid sprays or foams (Kovačević et al., 2022). Other common devices utilized for PAW production include pin-to-liquid discharge, DBD, gliding arc discharge, and microwave-induced discharge, as explained in Sections 2.1. to 2.5. These types of discharges produce distinct breakdown strengths in the gas phase and liquid, affecting the composition of RONS formed not only in the gaseous plasma but also in the liquid (Tachibana & Nakamura, 2019).

2.1 | Pin-to-liquid discharge

Generating an air pin-to-liquid discharge requires a pin as a high-voltage electrode positioned above the surface of the water and a ground electrode submerged in water as shown in Figure 1. The pin electrode can be made of metals, such as hafnium, copper, and stainless steel (Puertas et al., 2019). Yoon et al. (2018) studied the correlation between NTP and the gap distance during the generation of PAW via the pin-to-liquid discharge. The authors revealed that the formation of gaseous HNO_3 from the pin-to-liquid discharge caused a reduction in the surface tension of water. Increasing the activation time of the plasma discharge increased the conductivity of PAW and the discharge current, which were attributed to the transition of HNO_3 into H^+ and NO_3^- in the liquid (Yoon et al., 2018).

Decreasing the gap distance in the plasma discharge reduced the breakdown voltage and increased the discharge current, promoting higher mutual interactions between the plasma and the liquid and leading to higher reactive ions dissolving into the liquid (Yoon et al., 2018). Lim et al. (2022) found that the gap distance only influences the concentration of reactive oxygen species (ROS) in PAW, but not the reactive nitrogen species (RNS). Ng et al. (2021) indicated that the position of the ground electrode altered the chemistry of PAW, proving that having the ground electrode placed in the liquid produced high concentrations of NO_2^- and NO_3^- with undetected H_2O_2 concentration while having the ground electrode positioned beneath the liquid container generated high concentrations of H_2O_2 and NO_3^- with undetected NO_2^- concentration. It should be noted that the pin electrode might undergo electrode erosion because of evaporation, oxidation, melting, and sputtering (Puertas et al., 2019). When the initial liquid electric conductivity for the pin-to-liquid discharge increased, the concentrations of NO_2^- and NO_3^- increased (Hadinoto et al., 2021). Moreover, Liang et al. (2022) pointed out the importance of shielding the gas and the quartz tube that encloses the active electrode for improving the H_2O_2 and OH^- productions in PAW via the pin-to-liquid discharge. The authors found that

15414337, 0, Downloaded from https://ift.onlinelibrary.wiley.com/doi/10.1111/1541-4337.13250 by CochraneArgentina, Wiley Online Library on [13/10/2023]. See the Terms and Conditions (https://onlinelibrary.wiley.com/terms-and-conditions) on Wiley Online Library for rules of use; OA articles are governed by the applicable Creative Commons License

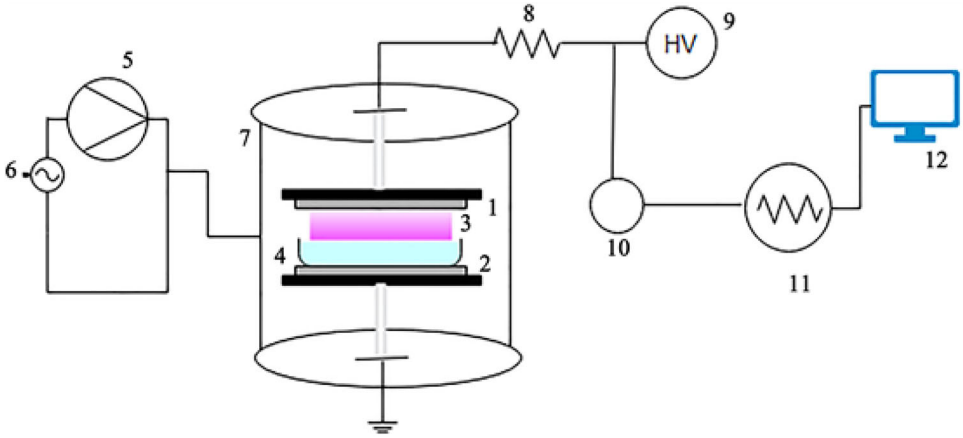

FIGURE 2 Schematic diagram of the dielectric barrier discharge setup: Electrodes (1, 2), Plasma discharge (3), Petri dish with water (4), Air pump (5), Power supply (6), Transparent cylinder (7), Ballast resistor (8), High-voltage supply (9), High-voltage probe (10), Shunt resistor (11), Computer (12). Reproduced from Shrestha et al. (2020) with the permission of Scientific Research Publishing Inc.

irrespective of the discharge gap (d_g), the discharge configuration with the shielding gas had the highest concentrations of H_2O_2 and OH^- in PAW in comparison with the other configurations.

2.2 | Dielectric barrier discharge

DBD typically involves a pair of electrodes with the presence of an insulating material or dielectric barrier, covering one of the electrodes or both, to avoid the formation of sparks in the discharge gap that can damage the electrodes (Neretti et al., 2016). DBD plasma interacts with water to produce PAW as shown in Figure 2. In addition, the discharge gap is filled with working gas, such as argon, helium, nitrogen, air, or their combinations (Anuntagool et al., 2023). The electric field applied to the gas must be sufficiently high to generate high-energy electrons that inelastic collide with surrounding gas molecules to generate plasma. The material of dielectric barrier can be made of ceramics, enamel, glass, plastics, quartz, silicon rubber, and Teflon, which limits the discharge current and minimizes energy consumption (Anuntagool et al., 2023; Brandenburg, 2017).

Tachibana and Nakamura (2019) estimated the energy yields of RONS production in PAW by using various DBD schemes, such as typical DBD, coaxial-DBD, monolithic mesh-type DBD, and water-sealed DBD. They found that only DBD and water-sealed DBD achieved high RONS energy yields, which were two to three times larger than other discharge schemes. A plasma jet with the discharge configuration of DBD favored high oxidizing potential, resulting in the high concentration of NO_3^- in PAW (Rathore & Nema, 2022). Moreover, Subramanian et al. (2021) demonstrated that H^+ and NO_3^-, which are the desired species in PAW generated by DBD, remained unchanged for up to 4 weeks.

2.3 | Gilding arc discharge

Generating a gliding arc discharge requires a high-velocity gas flowing between two or more divergent electrodes that are connected to a high-voltage power supply as shown in Figure 3 (Pawłat et al., 2019). The gas, such as humid air, pushes the formed arc plasma in the same direction along the axis of the reactor resulting in a series of sliding discharges that stretch across the inter-electrode region (Du et al., 2012; Mogo et al., 2022). Gliding arc plasma was reported to be rich in gaseous NO at up to 800 ppm and gaseous NO_2 at up to 200 ppm, which results in high productions of NO_2^- and NO_3^- in PAW (Pawłat et al., 2019). When the gas flowrate between the electrodes increases, it extends the length of the arc along the electrodes and requires a larger power to maintain the arc (Cho et al., 2023). However, the increased flowrate has an adverse impact on the NO_x concentration. It was reported that the lower the gas flowrate, the greater the NO_2 concentration produced in water (Cho et al., 2023). It was also found that increasing the voltage from 8 to 10 kV increased the NO_2^- and NO_3^- concentrations in PAW (Matra et al., 2022). Moreover, Guragain et al. (2023) found that temperature of distilled water did not change when the water was exposed with the gliding arc discharge for 5, 10, 15, and 20 min.

2.4 | Microwave-induced discharge

At the plasma–water interphase, surface-wave microwaves generate plasma discharge. Kaushik et al. (2023) reported

15414337, 0, Downloaded from https://ift.onlinelibrary.wiley.com/doi/10.1111/1541-4337.13250 by CochraneArgentina, Wiley Online Library on [13/10/2023]. See the Terms and Conditions (https://onlinelibrary.wiley.com/terms-and-conditions) on Wiley Online Library for rules of use; OA articles are governed by the applicable Creative Commons License

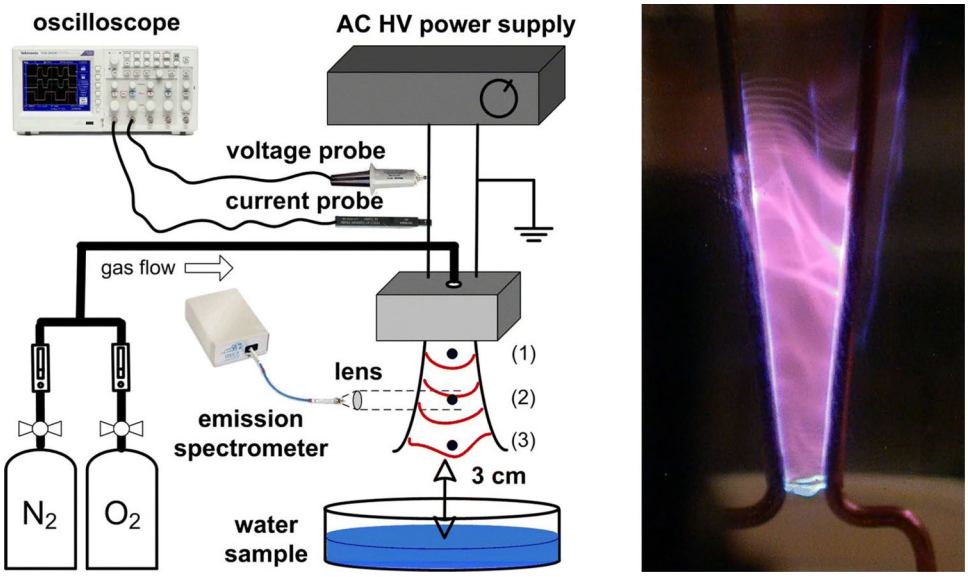

FIGURE 3 Schematic diagram of the gliding arc discharge and a photo of the reactor. Numbers (1, 2, 3) indicate the positions of measurement for emission spectra analysis. Reproduced from Pawlat et al. (2019) with the permission of Springer Nature.

the enrichment of NO during PAW production by using a microwave plasma system. They also reported that varying the initial gas mixture composition (Ar, $Ar/N_2/O_2$ binary, and ternary mixture) and the distance between the edge of the plasma-discharge tube and the water surface altered the electron and species densities at the interaction between the plasma and water. During the ageing of PAW generated via surface-wave microwave discharge, H_2O_2 was found to govern all the recombination of NO_2^- (Kaushik et al., 2023). Additionally, Lee et al. (2022) reported that H_2O_2 was undetected in PAW via the microwave plasma system; however, $ONOO^-$ was generated as an isomer of NO_3^-. Moreover, Kutasi et al. (2022) reported that adding metals, such as Mg or Zn, prior to PAW generation via a surface-wave microwave discharge can be beneficial, particularly in increasing the pH of PAW and maintain the RONS concentrations during storage.

2.5 | Multiphase discharge via bubbles

This is the discharge of plasma in gas bubbles that are immersed in water. This is a promising plasma configuration to minimize the loss of reactive species due to mass transfer limitations at the gas–water interface (Man et al., 2022; Ning et al., 2021). The gas composition, bubble formation, and bubble size influence the discharge pattern inside the bubble (Meropoulis & Aggelopoulos, 2023; Ning et al., 2021). Plasma bubbles promote the dissolution of reactive species, such as ozone, into the liquid because of their large interfacial areas, long residence time, and high internal pressures (Han et al., 2023; Zhou et al., 2021).

Mai-Prochnow et al. (2020) found that increasing the discharge frequency from 500 to 2000 Hz during the PAW production via plasma bubbles (Figure 4) increased the concentrations of OH^-, O_3, NO_2^-, NO_3^-, and H_2O_2. Hadinoto et al. (2021) evaluated the effect of ground-electrode position on the generated RONS for air plasma-bubble discharge in water. The authors found that when the initial conductivity was increased from 0 to 0.02 and to 0.2 $S.m^{-1}$ by adding NaCl prior to plasma discharge and the ground electrode was positioned on the outside of the reactor, the NO_2^-/NO_3^- ratio shifted toward NO_2^-. This is because the gas flow controls the gas residence time in the reactor and influences the coexistence of gaseous short-lived and long-lived species, resulting in the increased NO_2^- concentration and the reduced NO_3^- and H_2O_2 concentrations (Hadinoto et al., 2021). Man et al. (2022) developed an air microbubble plasma reactor with excellent energy efficiency to produce RONS in PAW at 10.4 $g.kW^{-1}.h^{-1}$ due to the enhanced electric field. Moreover, Gao et al. (2022) reported that the inclusion of microbubbles in plasma activation can result in over five times higher efficiency for dye degradation, in contrast to the setup without microbubbles.

Hadinoto, Rao, et al. (2023) assessed the effects of orifice diameter and number of holes regulating the size and number of bubbles injected into the liquid on the RONS formation during PAW generation via a hybrid plasma discharge as shown in Figure 5. This hybrid plasma discharge reactor was energy efficient with the value of 1.81 $\times$ 10^{-1} $mol.kW^{-1}.h^{-1}$ and achieved a high inactivation of 5.18 $\log_{10}$ reduction against planktonic bacteria within 30 s of contact time. This is because it induced high

15414337, 0, Downloaded from https://ift.onlinelibrary.wiley.com/doi/10.1111/1541-4337.13250 by CochraneArgentina, Wiley Online Library on [13/10/2023]. See the Terms and Conditions (https://onlinelibrary.wiley.com/terms-and-conditions) on Wiley Online Library for rules of use; OA articles are governed by the applicable Creative Commons License

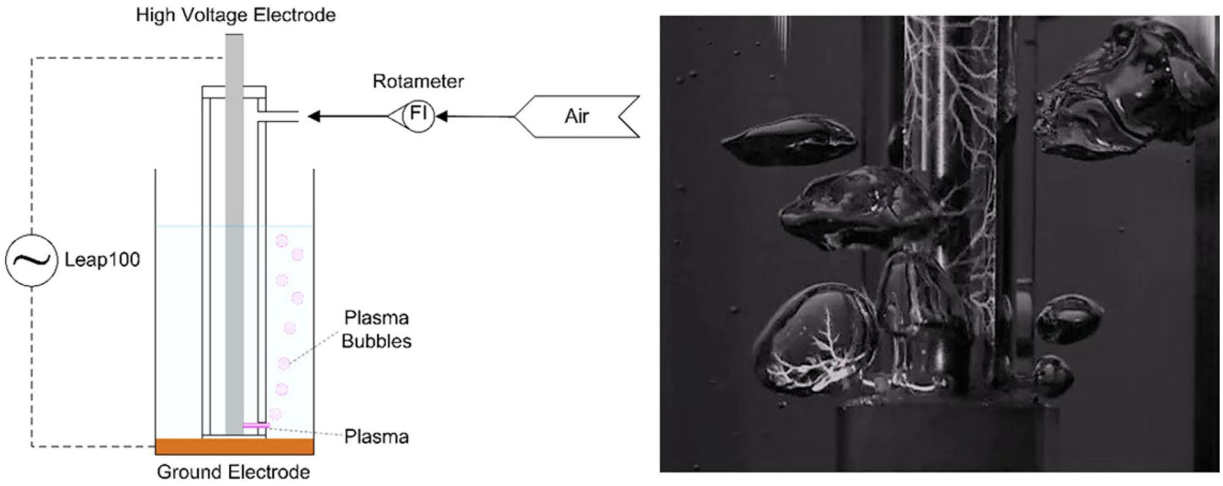

FIGURE 4 (a) Schematic diagram of the plasma-bubble generator. (b) Photograph of a discharge in a forming bubble. Reproduced from Mai-Prochnow et al. (2020) with the permission of John Wiley and Sons.

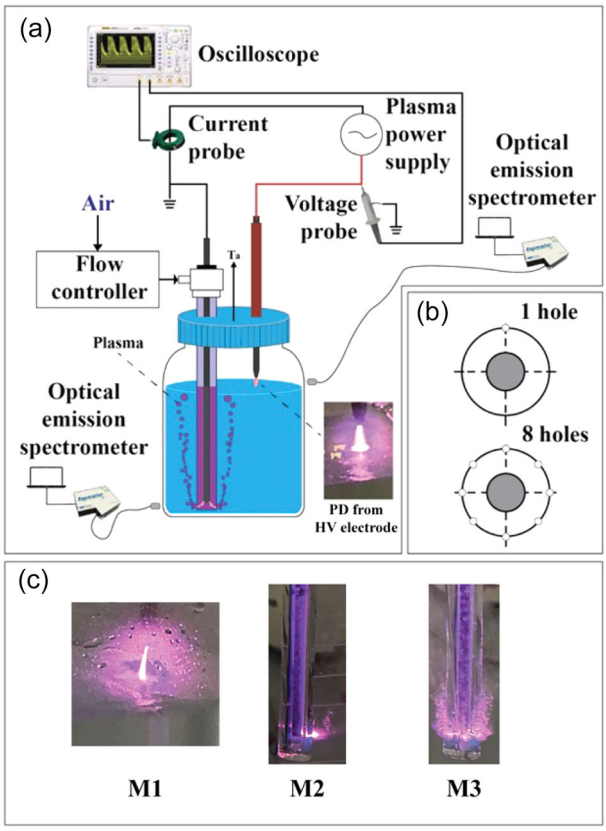

FIGURE 5 (a) Schematic illustration of the experimental setup of non-thermal plasma reactor for hybrid plasma discharge (HPD); (b) Cross-sectional view of the plasma-bubble column for the ground electrode of the HPD reactor; (c) images of the plasma discharge from the ground electrode of the HPD reactors with a single hole (M1, 2 mm); a single hole (M2, 400 μm), and eight holes (M3, 400 μm). T_a represents gas out to the atmosphere; PD represents plasma discharge. Reproduced from Hadinoto et al. (2023) with the permission of Elsevier.

electric fields not only at the high-voltage electrode but also at the ground, where plasma is discharged as plasma bubbles into the reactor, within one power source. The NO_2^- concentration decreased when the orifice diameter was changed from 2 mm to 400 μm because reducing the orifice diameter increased the number of bubbles at a constant air flowrate, which enhanced the mass transfer rate and increased the NO_3^- concentration attributed to the conversion of NO_2^- to NO_3^- along with the enriched gaseous O, O_2^-, and O_3 generation (Hadinoto, Rao, et al., 2023). When the number of orifices increased from one to eight holes, the NO_2^- concentration decreased and the NO_3^- concentration increased due to the increased generation of bubbles with a smaller diameter resulting in an increased rate of mass transfer with an increase in the dissolved O_3 concentration (Hadinoto, Rao, et al., 2023). Overall, integrating microbubbles with cold plasma can greatly improve the impregnation of active species generated from the plasma into the water, leading to a more efficient activation process.

3 | CHEMICAL PROPERTIES OF PAW

Zhou et al. (2018) revealed that positive ions (O^+, O_2^+, N^+, NO^+, NO_2^+, H_2O^+, H_3O^+, N_2^+, N_2H^+, N_2O^+) and negative ions (O^-, OH^-, O_2^-, O_3^-, NO_3^-, H_3O^-, $O^-(H_2O_2)$, CO_3^-, HCO_3^-) were generated in air plasma via a plasma jet. These positive and negative species can interact with water molecules, involving penetration, diffusion, and complex reactions that happen in the gas, in the liquid, and at the interface between the gas and the liquid. Through this process, ROS and RNS are formed in the liquid. This

15414337, 0, Downloaded from https://ift.onlinelibrary.wiley.com/doi/10.1111/1541-4337.13250 by CochraneArgentina, Wiley Online Library on [13/10/2023]. See the Terms and Conditions (https://onlinelibrary.wiley.com/terms-and-conditions) on Wiley Online Library for rules of use; OA articles are governed by the applicable Creative Commons License

topic has been briefly discussed by Zhou et al. (2020), Machala et al. (2019), Zhou et al. (2018), and Mohades et al. (2020). It should be noted that gases such as argon, oxygen, and nitrogen involve different reaction pathways to produce the gaseous excited species in plasma than air. The effect of gas type on the antimicrobial effect of PAW is discussed in Section 4.1.

For argon plasma, reaction pathways (1)–(3) are involved (Bolouki et al., 2021; Ghimire et al., 2021).

$$Ar + e \rightarrow Ar^{+} + e + e \quad (1)$$

$$Ar + e \rightarrow Ar^{*} + e \quad (2)$$

$$Ar^{*} + H_2O \rightarrow Ar + \cdot OH + H \quad (3)$$

For oxygen plasma, reaction pathways (4)–(9) are involved (Bolouki et al., 2021).

$$O_2 + e \rightarrow O^{+} + O + e \quad (4)$$

$$O_2 + e \rightarrow O^{-} + O \quad (5)$$

$$O + O_2 \rightarrow O_3 \quad (6)$$

$$O + H_2O \rightarrow 2 \cdot OH \quad (7)$$

$$OH^{-} + O_3 \rightarrow HO_2^{-} + O_2 \quad (8)$$

$$HO_2^{-} + O_3 \rightarrow \cdot OH + O_2^{-} + O_2 \quad (9)$$

For nitrogen plasma, reaction pathways (10)–(12) are involved (Bolouki et al., 2021).

$$N_2 + e \rightarrow N + N + e \quad (10)$$

$$N_2 + e \rightarrow N_2^{*} + e \quad (11)$$

$$N^{*} + H_2O \rightarrow N + \cdot OH + H \quad (12)$$

When air molecules (N_2 and O_2) are present in the feeding gas, chemical pathways (13)–(31) describe the possible chemical reactions on the formations of RONS in PAW (Beckman et al., 1990; Kučerová et al., 2020; Miller & Bowman, 1989; Pavlovich et al., 2014; Tachibana & Nakamura, 2019):

$$^{*}e + N_2/O_2 \rightarrow \cdot N + \cdot O + e \quad (13)$$

$$\cdot N + \cdot O \rightarrow \cdot NO \quad (14)$$

$$^{*}N_2 + \cdot O \rightarrow \cdot NO + \cdot N \quad (15)$$

$$O_2 + \cdot N \rightarrow \cdot NO + \cdot O \quad (16)$$

$$\cdot NO + \cdot O \rightarrow \cdot NO_2 \quad (17)$$

$$\cdot NO + O_2 \rightarrow \cdot ONOO \quad (18)$$

$$\cdot NO + \cdot ONOO \rightarrow ONOONO \rightarrow 2 \cdot NO_2 \quad (19)$$

$$\cdot NO + O_3 \rightarrow \cdot NO_2 + O_2 \quad (20)$$

$$\cdot NO_2 + \cdot O + M \rightarrow \cdot NO_3 + M\,(N_2 \text{ or } O_2) \quad (21)$$

$$\cdot NO_2 + O_3 \rightarrow \cdot NO_3 + O_2 \quad (22)$$

$$2NO_{2aq} + H_2O \rightarrow NO_2^{-} + NO_3^{-} + 2H^{+} \quad (23)$$

$$4NO_{2aq} + O_{2aq} + 2H_2O \rightarrow 4NO_3^{-} + 4H^{+} \quad (24)$$

$$NO_{2aq} + OH_{aq} \rightarrow NO_3^{-} + H^{+} \quad (25)$$

$$NO_2^{-} + O_{3aq} \rightarrow NO_3^{-} + O_{2aq} \quad (26)$$

$$NO_2^{-} + H_2O_2 \rightarrow NO_3^{-} + H_2O \quad (27)$$

$$3NO_2^{-} + 3H^{+} \rightarrow 2NO_{2aq} + NO_3^{-} + H_2O + H^{+} \quad (28)$$

$$NO_2^{-} + NO_{3aq} \rightarrow NO_3^{-} + NO_{2aq} \quad (29)$$

15414337, 0, Downloaded from https://ift.onlinelibrary.wiley.com/doi/10.1111/1541-4337.13250 by CochraneArgentina, Wiley Online Library on [13/10/2023]. See the Terms and Conditions (https://onlinelibrary.wiley.com/terms-and-conditions) on Wiley Online Library for rules of use; OA articles are governed by the applicable Creative Commons License

$$H_2O + e^- \rightarrow H + \cdot OH + e^- \quad (30)$$

$$\cdot OH + \cdot OH \rightarrow H_2O_2 \quad (31)$$

$$NO_{aq} + NO_{2aq} + H_2O \rightarrow 2NO_2^- + 2H^+ \quad (32)$$

$$NO_2^- + H^+ \rightarrow HNO_2 \quad (33)$$

$$HNO_2 + H^+ \rightarrow NO^+ + H_2O \quad (34)$$

$$2HNO_2 \rightarrow \cdot NO + \cdot NO_2 + H_2O \quad (35)$$

$$NO_2^- + H_2O_2 + H^+ \rightarrow O = NOOH + H_2O \quad (36)$$

$$HNO_2 + H_2O_2 \rightarrow O = NOO^- + H_2O \quad (37)$$

Pathways (13)–(16) show the formation of nitric oxide with plasma excitation of atmospheric air, with the first step as the formation of NO_x ($x = 2, 3$) species in the gas phase. ·NO and ·N species in the gaseous state are formed via the rate-limiting reaction between N_2 and ·O (Miller & Bowman, 1989). ·NO species are also formed via the reaction of O_2 with ·N, and the reaction between N_2 and ·OH via the electron-impact dissociation of water vapor in atmospheric air (Miller & Bowman, 1989). The NO_x formations occur via the oxidation reactions of the primary species ·NO as shown in pathways (17)–(22) (Pavlovich et al., 2014). ·NO_3 species can be formed via pathway (9), which is a collision between ·NO_2, ·O and a third body M (N_2 or O_2). It is reported that gaseous NO_x species undergo pathways (23)–(25) and (32) when transferred into water (Tachibana & Nakamura, 2019). Gaseous ·NO and ·NO_2 species can dissolve in water to generate NO_2^-, NO_3^-, and H^+ through the involvement of oxidizing species such as ·O, O_2, O_3, and ·OH (Xiang et al., 2018).

The ionic pathways (26)–(29) are also believed to occur during the conversion of NO_2^- to NO_3^- (Tachibana & Nakamura, 2019). H_2O_2 can be formed via the electron–water interactions at the gas–water interface, shown in reactions (30) and (31). NO and NO^+ species can be formed through the decomposition of unstable HNO_2 (Zhou et al., 2018), in pathways (33)–(35). Under a pH of 3.3, NO_2^- and H_2O_2 undergo pathway (36) to form O = NOOH, or at higher pH, O = NOO^- can be formed (Zhou et al., 2018). From the chemical pathways above, nitrite (NO_2^-), nitrate (NO_3^-), hydrogen peroxide (H_2O_2), and ozone (O_3), have been widely accepted as the long-lived RONS in PAW and hydroxyl radical (•OH), superoxide (•O_2^-), and peroxynitrite (O = NOO^-) as the short-lived RONS, which also have major impacts in the conductivity, pH, and redox potential of PAW. Hence, quantifying these species and comprehending their chemical pathways in solution is important in expanding the application and commercial potential of PAW.

It is known that PAW has a rich diversity of RONS that increases the liquid conductivity, decreases the pH, and impacts the oxidation–reduction potential (ORP) (Jin et al., 2020). The conductivity of PAW reflects the ability of the solution to conduct electric current (Subramanian et al., 2021). The nitrous and nitric acids formed during the interaction between plasma and water cause a decrease in the pH of PAW (Rathore & Nema, 2022). Shen et al. (2016) showed that PAW reduced the pH of water from 6.8 to 2.3, indicating a higher amount of hydrogen cation (H^+) in the solution, attributed to reaction pathways (11)–(13). The ORP values indicate the electron transfer ability through chemical reactions in PAW (Bolouki et al., 2021).

When air humidity increases with an increase in the activation time of PAW, ozonoid (O_3^-) can be produced instead of O_3, which subsequently is converted to ·OH in the gas phase (Perinban et al., 2022). When the pH of the liquid solution is below 6 during plasma discharge, the degradations of H_2O_2 and O_3 in the liquid phase are favored to form hydroperoxide ion (HO_2^-) via pathways (40)–(46) (Perinban et al., 2022).

$$O_3 + e^- \rightarrow O_3^- \quad (38)$$

$$O_3^- + H_2O \rightarrow \cdot OH + OH^- + O_2 \quad (39)$$

$$H_2O_2 + O_3 \rightarrow 2 \cdot OH + O_3^- \quad (40)$$

$$H_2O_2 \rightarrow \cdot HO_2^- + H^+ \quad (41)$$

$$\cdot HO_2^- \rightarrow H^+ + O_2^- \quad (42)$$

$$O_2^- + O_3 \rightarrow O_2 + O_3^- \quad (43)$$

$$O_3^- + H^+ \rightarrow HO_3 \quad (44)$$

$$HO_3 \rightarrow \cdot OH + O_2 \quad (45)$$

$$\cdot OH + O_3 \rightarrow \cdot HO_2^- + O_2 \quad (46)$$

15414337, 0, Downloaded from https://ift.onlinelibrary.wiley.com/doi/10.1111/1541-4337.13250 by CochraneArgentina, Wiley Online Library on [13/10/2023]. See the Terms and Conditions (https://onlinelibrary.wiley.com/terms-and-conditions) on Wiley Online Library for rules of use; OA articles are governed by the applicable Creative Commons License

4 | MICROBIAL INACTIVATION BY PAW

A variety of plasma sources to produce PAW have been successfully proven to inactivate a variety of planktonic bacteria, as summarized in Table 1. This poses PAW as an attractive alternative to traditional techniques for bacterial inactivation. It is commonly accepted that the RONS in PAW attribute to the antimicrobial efficacy of PAW, attacking unsaturated fatty acids in the cell membrane and resulting on lipid oxidation (Man et al., 2022; Su et al., 2018; Zhao et al. (2020a). Rivero et al. (2022) proposed that the synergetic effect of NO_2^-, $ONOO^-$, and low pH leads the destruction of bacterial cells. However, few researchers have proposed that the ROS in PAW are also responsible for the microbial inactivation of PAW by initiating lipid peroxidation in the cell membrane (Gan et al., 2022; Perinban et al., 2022). Han et al. (2022) reported that $\bullet O_2^-$ has a key role in the mechanism of antimicrobial inactivation induced by PAW while NO_2^- and NO_3^- with pH drop acted as the supporting agents in the inactivation. •OH also plays a role in the bacterial inactivation by oxidizing unsaturated fatty acids in the cell membrane, cleaving peptide bonds, and oxidizing amino acid side chains (Guo et al., 2023).

It is accepted that the microbial inactivation of PAW is due to a combination of its RONS and low pH. The ORP of PAW could also be an important factor affecting PAW inactivation (Kasih et al., 2022). Bai et al. (2020) noted that the initial concentration of bacteria affects the bacterial resistance to PAW treatment, revealing that the higher the bacterial load, the lower the inactivation rate.

For in situ PAW treatment, Rothwell et al. (2022) investigated the use of scavengers, such as mannitol (which scavenges •OH), hemoglobin (which scavenges NO), sodium pyruvate (which scavenges H_2O_2), tiron (which scavenges $\bullet O_2^-$), and uric acid (which scavenges O_3), to identify which reactive species in PAW contributed to the antimicrobial activity of PAW against *Listeria innocua* and *E. coli*. The authors revealed that $\bullet O_2^-$ is the only species affecting the inactivation. Similarly, Xia et al. (2023) reported that the oxygen toxicity of $\bullet O_2^-$ radicals in PAW generated using oxygen are responsible for the removal of *E. coli* biofilms. Other authors reported that the $ONOO^-$ species in PAW was the main factor inducing the antimicrobial effect (Ikawa et al., 2016; Zhou et al., 2018). $ONOO^-$ can directly react with protein molecules in bacteria through hydrogen abstraction, coupling, oxygenation, and cleavage (Guo et al., 2023).

4.1 | Microbial inactivation mechanisms

In general, the mechanisms associated with PAW inactivation against bacteria involves multiple phases as shown in Figure 6. The bacterial cell envelope is the main target when PAW interacts with bacteria. The RONS generated in PAW (i) induces cell permeability and forms transient pores due to electroporation, which promotes the RONS entering the cells, (ii) initiates lipid peroxidation in the cell membrane by disturbing the chemical bonds of the cell membrane, which is mainly composed of lipids, phospholipids, fatty acids, and proteins of the cell membrane (Liu et al., 2021a; Zhang et al., 2016). Damaging the cell membrane increases the difficulty of cellular homeostasis. In addition, the extracellular RONS travelling across the transient opening of pores in the cell membrane and the oxidative stress in the bacterial cells induced by the external oxidative stress create the enlargement of intracellular RONS (Ma et al., 2013; Zhang et al., 2016). The increased intracellular RONS leads to cell death by oxidizing DNA in the nucleus as well as damaging intracellular organelles and enzymes (Ma et al., 2013; Zhang et al., 2016). Moreover, the intracellular pH and intracellular RONS induce the interference of intracellular pH homeostasis, which leads to physiological dysfunctions of the bacterial cells and irreversible cell damage (Guo et al., 2022; Zhang et al., 2016).

The characteristic of bacteria, including their nature and cellular structure, is a critical factor impacting the inactivation mechanism of PAW. Zhao et al. (2020a) reported that the PAW inactivation against *L. innocua* and *S. aureus* as Gram-positive species were lower than those against Gram-negative species (*E. coli*, *Aeromonas hydrophila*, *Pseudomonas fluorescens*, and *Shewanella putrefaciens*), attributed to higher protection with denser cell wall for Gram-positive bacteria. Gram-positive bacteria have a cell wall thickness of 20–80 nm, which is thicker than the cell wall of Gram-negative bacteria at less than 10 nm (Wang & Salvi, 2021). In addition, *S. aureus* cells were reported to be less prone to irreparable oxidative damage by PAW treatment in comparison with *L. innocua*, due to the resistance mechanisms that they acquire (Zhao et al., 2020a). Jyung et al. (2022) measured reactive species in PAW diffused into Gram-positive bacteria, revealing that the thick peptidoglycan layer of Gram-positive bacteria acted as a physical shield and increased the bacterial resistance to PAW compared to Gram-negative bacteria. Xiang et al. (2018) also indicated that PAW damaged the cell wall and membrane of *Pseudomonas deceptionensis* CM2 with up to 155% and 161% of the extracellular nucleic acid and proteins, respectively, in comparison with the untreated bacterial samples.

Although the structure of the cell envelope is an important factor in microbial defense in PAW treatment, the shape of the bacterial cell is the other contributing aspect that needs to be considered (Simoncicova et al., 2019). The behavior of PAW inactivating bacterial cells is also influenced by the treatment time of PAW. Based on the images

15414337, 0, Downloaded from https://ift.onlinelibrary.wiley.com/doi/10.1111/1541-4337.13250 by CochraneArgentina, Wiley Online Library on [13/10/2023]. See the Terms and Conditions (https://onlinelibrary.wiley.com/terms-and-conditions) on Wiley Online Library for rules of use; OA articles are governed by the applicable Creative Commons License

TABLE 1 Recent studies on plasma-activated water inactivation against planktonic bacteria.

	Activation conditions			Inactivation efficacy				
Plasma source	**Volume of liquid**	**Discharge conditions**	**Activation time**	**Bacteria**	**Initial load (log_{10} CFU.mL^{-1})**	**Maximum log_{10} reduction CFU.mL^{-1}**	**Treatment time**	**Reference**
Plasma jet	200 mL	Air, 22.5 kHz, 295 V	1-15 min	*Escherichia coli*, *Listeria innocua*	6	>5.00	5 min	Wang and Salvi (2021)
Arc discharge	40–70 mL.min^{-1}	20 kHz, 2 kV	–	*Listeria monocytogenes*, *Escherichia coli*	7	4.13	1–5 min	Baek et al. (2020)
Plasma jet	200 mL	Air, 750 W	30–90 s	*Pseudomonas deceptionensis* CM2	8-9	5.00	10 min	Xiang et al. (2018)
Plasma jet	20 mL	Ar/O_2, 10 kHz, 18 kV	20 min	*Staphylococcus aureus*	–	6.00	10 min	Zhang et al. (2013)
DBD	15 mL	Air, 20 kHz, 100 kV	5 min	*Staphylococcus aureus*	9	2.50	5 min	Wu et al. (2017)
Gliding arc discharge	200 mL	Air, 40 kHz, 5 kV, 750 W	60 s	*Escherichia coli*	8	0.77	4 min	Xiang et al. (2019)
Plasma jet	50–100 mL	Air, 650 W	60 s	*Bacillus cereus*	6	2.96	60 min	Bai et al. (2020)
Plasma jet	50 mL	Air	5–30 min	*Escherichia coli*	8	4.00	10 min	Zhou et al. (2018)
Plasma array source	5 mL	Air, 5 kHz, 18 kV	300 s	*Escherichia coli*	10	10	5 min	Ma et al. (2020)
Plasma jet	30 mL	Air, 15–30 kV	5 min	*Escherichia coli*, *Listeria innocua*, *Staphylococcus aureus*, *Aeromonas hydrophilia*, *Shewanella putrefaciens*, *Pseudomonas fluorescens*	6–8	>5	0.5–24 h	Zhao et al. (2020a)
DBD	100 mL	Air, 80 kV, 400 W	–	*Listeria innocua*, *Escherichia coli*	6	>6	1–2 min	Rothwell et al. (2022)

15414337, 0, Downloaded from https://ift.onlinelibrary.wiley.com/doi/10.1111/1541-4337.13250 by CochraneArgentina, Wiley Online Library on [13/10/2023]. See the Terms and Conditions (https://onlinelibrary.wiley.com/terms-and-conditions) on Wiley Online Library for rules of use; OA articles are governed by the applicable Creative Commons License

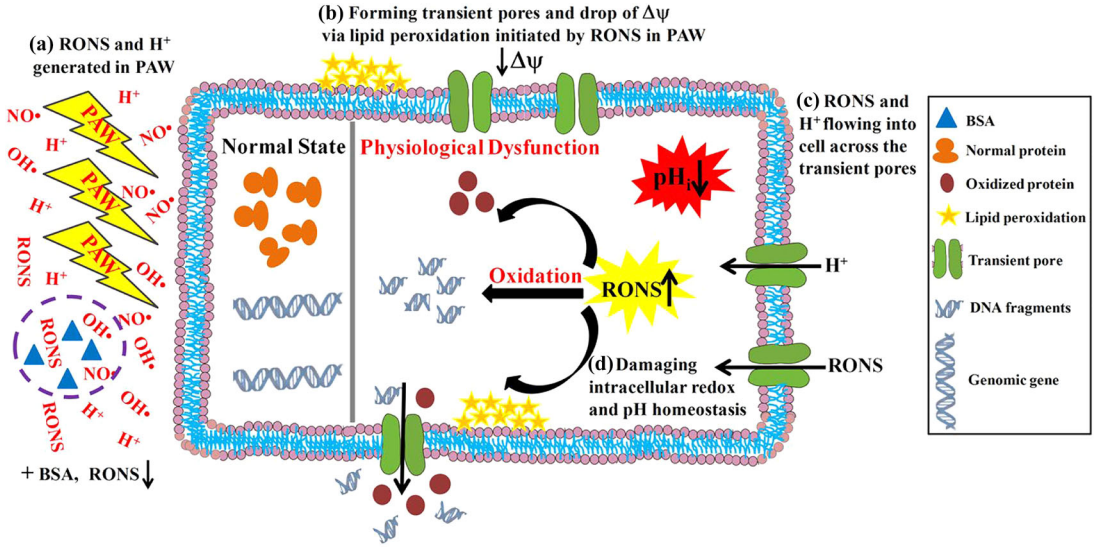

FIGURE 6 Schematic diagram of the microbial inactivation induced by plasma-activated water (PAW). The authors noted that the addition of bovine serum albumin (BSA) during plasma discharge decreased the reactive nitrogen and oxygen species produced in PAW. Reproduced from Zhang et al. (2016) with the permission of American Chemical Society.

of transmission electron microscopy (TEM) obtained by Baek et al. (2020), PAW damaged the outer shell of Gram-positive bacteria at the treatment time of 1 min and injured the intracellular components of the cells, such as nucleic acids and proteins, at 5 min while the cell structure of PAW-treated Gram-negative bacteria was dramatically changed. Furthermore, the increased reactive species in PAW with the increased discharge frequency or output voltage gradually increased the permeability of the cell membrane (Asimakopoulou et al., 2022; Zhao et al., 2020a).

4.2 | Processing factors influencing inactivation effectiveness

The antimicrobial activity of PAW depends on the mode of plasma generation, activation time, dose of energy input, treatment time and the characteristics of microorganism, which has been discussed in the published literature (Herianto et al., 2021; Xiang et al., 2022; Zhao et al., 2020a). There are many processing factors that influence the antimicrobial effectiveness of PAW, including working gas type, gas flowrate, storage time, storage temperature, water type, water conductivity, and liquid temperature. Understanding these factors are crucial for the technology translation at the industrial scale.

4.2.1 | Working gas type and its flowrate

Gas type plays a dominant role in the formation of reactive species at the plasma–liquid interaction and bacterial inactivation of PAW. Bolouki et al. (2021) investigated the effects of various gases, such as air, nitrogen, oxygen, and argon, on the physiochemical properties of PAW generated via DBD at the treatment times of 2, 4, 6, 8, 10, and 12 min; optical emission spectroscopy (OES) revealed that different spectra patterns and relative intensities of the gaseous reactive species were generated during the interaction between plasma and liquid when using different types of working gases. For the plasma generated with air and nitrogen, the pH of PAW decreased with the increased treatment time; however, the pH was not significantly changed for the plasma treatment with argon and oxygen because of the absence of nitrogen species (Bolouki et al., 2021).

Compared to other gases, air produced the highest concentrations of RNS, including nitrite and nitrate, in PAW at activation times higher than 10 min while oxygen exhibited the highest concentration of hydrogen peroxide. Interestingly, Mohades et al. (2020) reported, specifically for PAW generated via DBD, that argon as the feeding gas produced the highest H_2O_2 concentration in the solution whereas air produced the highest aqueous •OH concentration and oxygen produced the highest dissolved O_3 concentration. Moreover, changes in PAW chemistry contributed to the overall antimicrobial effect of PAW with different chemical reactions controlling the RONS production in the liquid. Zhou et al. (2018) indicated that adopting air as the working gas is more desirable for the implementation of PAW in the food industry because it is abundant and low cost.

Machala et al. (2019) pointed out the importance of the air flow rate in the chemical composition of PAW,

15414337, 0, Downloaded from https://ift.onlinelibrary.wiley.com/doi/10.1111/1541-4337.13250 by CochraneArgentina, Wiley Online Library on [13/10/2023]. See the Terms and Conditions (https://onlinelibrary.wiley.com/terms-and-conditions) on Wiley Online Library for rules of use; OA articles are governed by the applicable Creative Commons License

especially in the formation rates of gaseous RONS. It is important to recognize that the flow rate of gas is not always in a positive relationship to the inactivation of PAW. The gas flow rate regulates the residence time of gas feeding into the plasma system and the plasma intensity to produce reactive species in the gas phase (Perinban et al., 2022). Machala et al. (2019) showed that the concentrations of nitric oxide and nitrite in the gas plasma increased at the lowest air flow rate because of larger accumulated reactive species in the closed reactor at the lowest flow rate.

Hadinoto et al. (2021) evaluated the impact of varying air flow rates on both the energy efficiency and the bacterial inactivation of a plasma-bubble reactor. Their findings indicated that increasing the airflow from 0.2 to 0.8 L.min^{-1} (which was the optimal flow rate at a discharge frequency of 2000 Hz) resulted a rise of RONS energy efficiencies from 4.25 to 8.60 g kW^{-1} h^{-1}. This increase can be attributed to the higher concentration of active species introduced into the reactor at the optimal flow rate, which in turn raised the NO_3^- concentration. However, the survived populations of *E. coli* were decreased when the airflow changed from 0.2 to 0.8 L.min^{-1}.

Royintarat et al. (2019) varied the composition of a mixture of argon (Ar) and oxygen (O_2), at 98%, 99%, and 100% Ar, with the gas flowrates of 2, 4 and 6 L min^{-1} for the *E. coli* and *S. aureus* inactivation of PAW via a cylindrical DBD plasma reactor. They found that the optimal inactivation, at 0.45 and 2.45 log$_{10}$ reduction CFU.mL^{-1} against *E. coli* and *S. aureus*, respectively, was achieved with 99% Ar (and 1% O_2) at 4 L.min^{-1} for 11.5 min of treatment. Shaw et al. (2018) revealed that the gas mixture of nitrogen and 0.5 wt% of vapor nitric acid led to the highest antimicrobial inactivation of PAW against *E. coli* compared to other gas mixtures, such as nitrogen and nitrogen with water vapor. In addition, Ali et al. (2021) showed that in comparison with a gas mixture of argon and oxygen, higher reductions of chlorothalonil and thiram pesticide residues on tomato were achieved by PAW when the air was introduced during plasma discharge, which is associated with the enhanced RONS production in PAW when using air as the working gas. Moreover, using air as the working gas during the discharge achieves higher RONS energy efficiency, offering significant economic viability over pure gases. For example, the energy efficiency generated via air was 2.24 times higher than those via argon (Cubas et al., 2021).

4.2.2 | Storage time and temperature

Storage time and temperature are crucial factors to govern the storability of PAW and the post-discharge stability of RONS in PAW, which consequently affect the microbial inactivation efficiency of PAW. Tsoukou et al. (2020)

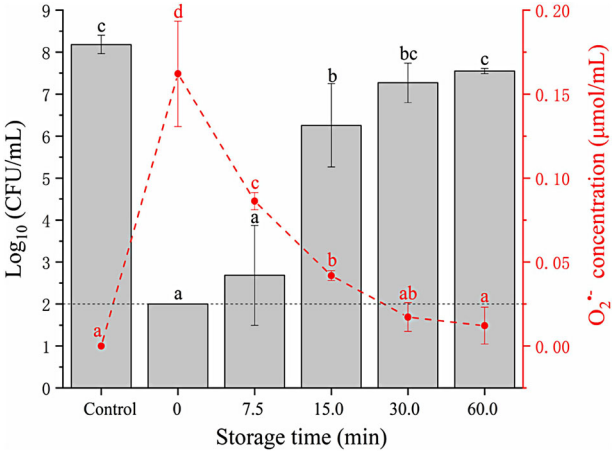

FIGURE 7 Plasma-activated water inactivation against *Escherichia coli* and concentration of superoxide anion radical ($O_2^{\cdot}-$) at different storage times. Reproduced from Han et al. (2022) with the permission of John Wiley and Sons.

investigated the effect of storage stability on the inactivation of PAW against planktonic *E. coli* and *S. aureus* cells by storing PAW at 20 (room temperature, RT), 4, −16, −80, and −150°C for up to 18 months prior to treating bacterial cells. The authors found that highest inactivation was achieved at 6 log$_{10}$ reduction CFU·mL^{-1} when PAW was stored at −80 and −150°C for 18 months. Storing PAW, for example at −16°C for a week, resulted in 3.00 to 4.00 log$_{10}$ reduction CFU.mL^{-1} while increasing the PAW storage time for another week decreased the inactivation to about 2.00 log$_{10}$ reduction CFU.mL^{-1}. These findings were associated with the stability of ROS and nitrate in PAW during storage (Tsoukou et al., 2020).

Shen et al. (2016) demonstrated that storing PAW at −80°C for up to 30 days achieved higher inactivation against *S. aureus* at 3 to 4 log$_{10}$ reduction CFU mL^{-1} compared to those at temperatures of 25, 4, and −20°C, due to its preserved concentrations of hydrogen peroxide and nitrite. Wang and Salvi (2021) examined the storage stability of PAW prepared using an air plasma jet. The authors indicated that increasing the storage time decreased both (i) the concentration of nitrate in PAW and (ii) the PAW microbial reductions against *E. coli* and *L. innocua*, irrespective of the storage temperature. In addition, the storage temperature of 4°C maintained the inactivation efficacy of PAW higher than at 22°C (Wang & Salvi, 2021).

Han et al. (2022) evaluated the influence of storage times at 7.5, 15, 30, and 60 min at room temperature during the PAW inactivation efficacy against planktonic *E. coli*. The authors reported that more than 6.18 log$_{10}$ reduction CFU.mL^{-1} of PAW was achieved with the storage time of 7.5 min (Figure 7). However, when the storage time reached 30 min, the inactivation decreased (Figure 7),

15414337, 0, Downloaded from https://ift.onlinelibrary.wiley.com/doi/10.1111/1541-4337.13250 by CochraneArgentina, Wiley Online Library on [13/10/2023]. See the Terms and Conditions (https://onlinelibrary.wiley.com/terms-and-conditions) on Wiley Online Library for rules of use; OA articles are governed by the applicable Creative Commons License

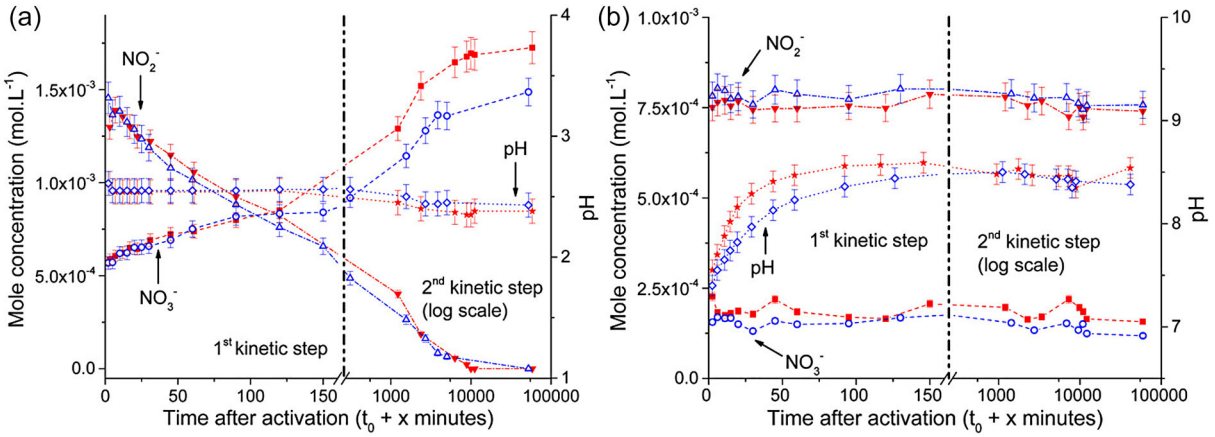

FIGURE 8 Evolution of the nitrate/nitrite (NO_3/NO_2) mole concentrations and pH as function of the time after activation of plasma-activated water prepared with (a) distilled water and (b) tap water via a gliding arc discharge. The plotted data in red (full symbols) concern the first test and the data in blue (empty symbols) for the second attempt. Reproduced from Wartel et al. (2021) with the permission of AIP Publishing.

which was attributed to the decrease of superoxide anion radicals as they are important inactivation agents in PAW (Han et al., 2022).

Perinban et al. (2022) revealed that the concentrations of hydrogen peroxide and ozone had an inverse proportional correlation with the storage time of PAW. The authors showed that the inactivation of planktonic bacterial cells decreased by 30%–50% after storing for 2 days. For the scalability of PAW in the food industry, Zhao et al. (2020a) recommended that the antimicrobial activity of PAW could last up to 24 h after its generation.

4.2.3 | Type of water and water conductivity

Many studies have reported that PAW production using different types of water, including deionized water, distilled water, tap water, and reverse osmosis water affects the PAW antimicrobial effectiveness. Wartel et al. (2021) noted that the post-discharge reactions on the concentration profile behavior of nitrite and nitrate during the PAW generation via a gliding arc discharge with distilled water were different to tap water. Figure 8a shows degradation of nitrite with an increase in the mole concentration of nitrate during the storage time. In contrast, the concentrations of nitrite and nitrate in PAW prepared with tap water were unaffected by the storage time (Figure 8b) because of the absence of acidification and the buffer effect of carbonates in tap water (Wartel et al., 2021). Moreover, it was reported that PAW (pH = 3.5) prepared from tap water performed the best inactivation efficacy against *E. coli* compared to distilled, deionized, filtered, and saline water as shown in Figure 9 (Sampaio et al., 2022).

Schmidt et al. (2019) compared the productions of PAW generated by a multi-pins-to-liquid discharge with different properties of treating liquid, including distilled water, tap water, and distilled water with 0.85% NaCl. They found that PAW prepared with tap water performed the best in terms of the inactivation efficacy of PAW against *E. coli* and *S. aureus*. Interestingly, Simon et al. (2021) investigated the effects of potable water collected from France, Norway, Palestine, Slovenia, and the United Kingdom on the generation of PAW. After plasma discharge, all water samples collected from these five countries increased the concentration of nitrate in PAW. Interestingly, only water from France and Palestine retained the pH of PAW at 8. The authors then evaluated the antimicrobial efficiency of PAW prepared from the United Kingdom and Palestine's water samples against *E. coli* and *S. aureus*, which revealed that PAW prepared with the UK's water samples achieved more than 6.00 $\log_{10}$ reduction $CFU.mL^{-1}$ while those with Palestine's samples reached 0.40 $\log_{10}$ reduction $CFU.mL^{-1}$ (Simon et al., 2021). These findings highlighted the importance of having appropriate water composition for future PAW development, as it affects its efficacy and repeatability.

Hadinoto et al. (2021) and Hadinoto et al. (2023) proved the importance of adding NaCl prior to plasma discharge, enhancing the bacterial inactivation. Increasing salinity increased the electric field and the total concentration of RONS in PAW (Hadinoto et al., 2023). Increasing the NaCl concentrations to more than 4 mM during the generation of PAW via a hybrid plasma discharge resulted >4 $\log_{10}$ reduction at a contact time of 30 s compared to the 3.19 $\log_{10}$ reduction achieved with non-saline PAW for the same contact time (Hadinoto et al., 2023).

15414337, 0, Downloaded from https://ift.onlinelibrary.wiley.com/doi/10.1111/1541-4337.13250 by CochraneArgentina, Wiley Online Library on [13/10/2023]. See the Terms and Conditions (https://onlinelibrary.wiley.com/terms-and-conditions) on Wiley Online Library for rules of use; OA articles are governed by the applicable Creative Commons License

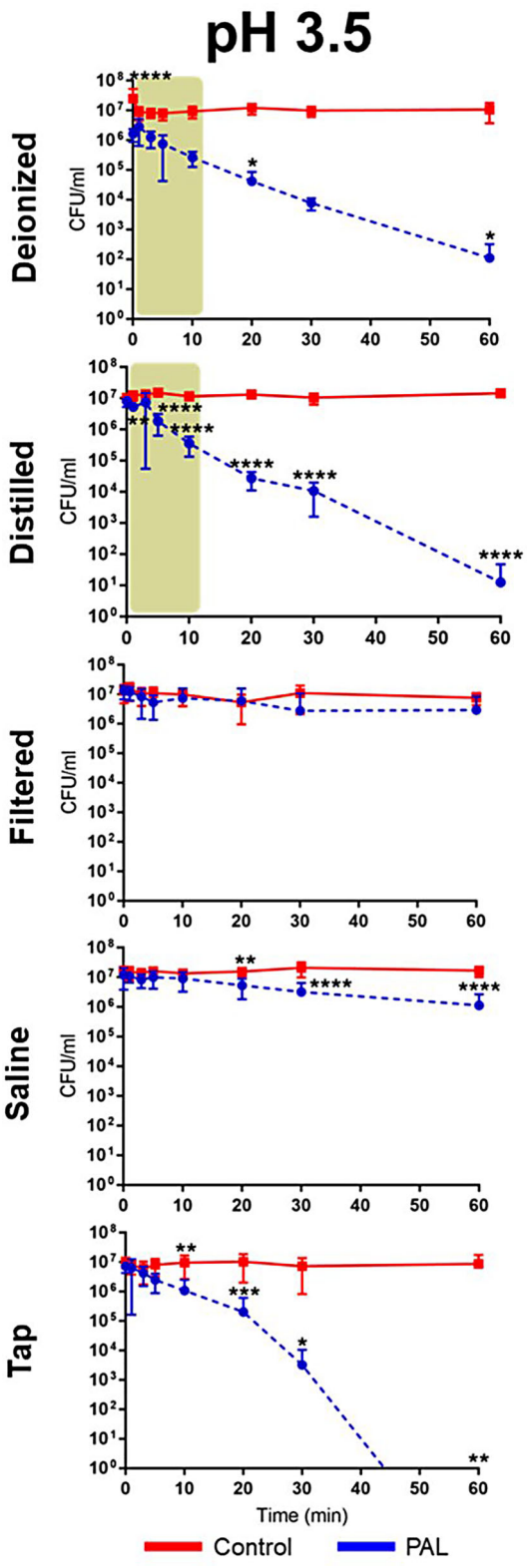

FIGURE 9 Overview of the antibacterial effects of *Escherichia coli* exposure in contact with plasma-activated water prepared from distilled, deionized, filtered, 0.9% saline and tap water over time at pH = 3.5. Reproduced from Sampaio et al. (2022) with the permission of MDPI.

4.2.4 | Liquid temperature

The initial liquid temperature for PAW generation affects the production of RONS and the antimicrobial effectiveness of PAW. Pang et al. (2021) shows the effects of initial liquid temperatures at 4, 25, 40, and 70°C on the chemical characteristics of PAW generated via an atmospheric plasma jet with the activation time of 10 min and a mixture of 99.5% helium and 0.5% nitrogen as the working gas. The optimal liquid temperature was 25°C because temperatures above 25°C decreased the amount of RONS produced in PAW, which was associated with the water evaporation at 40 and 70°C impacting the intensity of plasma discharge, the liquid density, surface tension, and the reaction rates of RONS in PAW.

The solubility of oxygen and other gasses during plasma generation also decreased as the liquid temperature increased; consequently, lower solubility of NO_x was induced (Pang et al., 2021). In addition, Pang et al. (2021) revealed that the increased liquid temperature from 25 to 70°C reduced the apoptosis rate of cancer cells by flow cytometry from 27.1% to 12% due to a higher concentration of RONS in PAW at 25°C. Moreover, Man et al. (2022) assessed the effect of controlling the liquid temperature at the values of 10, 20, and 37°C during the direct PAW treatment against *E. coli* at the treatment times of 1, 3, and 5 min, concluding that PAW treatment at the liquid temperature of 10°C achieved the highest inactivation efficacy of 2.43 $\log_{10}$ reduction CFU.mL^{-1} because of its highest formation of aqueous ozone.

5 | APPLICATIONS OF PAW FOR MEATS AND MEAT PRODUCTS

5.1 | Curing of meat products using PAW

PAW provided a new avenue to produce an alternative nitrite source for meat curing (Inguglia et al., 2020). Inguglia et al. (2020) produced PAW by a plasma-beam system at 20 kHz for 10 min using four solutions with sodium nitrite concentrations at 0, 50, 100, and 150 ppm. PAW treatment resulted in 0.85 $\log_{10}$ reduction CFU g^{-1} in *L. innocua* on beef jerky compared to conventional curing methods at 50 and 150 ppm of sodium nitrite, with no significant impact on the lipid oxidation and texture of the samples. This was due to the presence of nitrite in the PAW solution, increasing the antimicrobial effectiveness (Inguglia et al., 2020).

Meanwhile, Kim et al. (2016) revealed that the emulsion-type sausage cured with PAW did not cause mutagenicity

15414337, 0, Downloaded from https://ift.onlinelibrary.wiley.com/doi/10.1111/1541-4337.13250 by CochraneArgentina, Wiley Online Library on [13/10/2023]. See the Terms and Conditions (https://onlinelibrary.wiley.com/terms-and-conditions) on Wiley Online Library for rules of use; OA articles are governed by the applicable Creative Commons License

and immune toxicity of meat products. Yong et al. (2018) generated PAW via DBD with an activation time of 2 h for the curing of lion ham, achieving <0.5 $\log_{10}$ reduction CFU g^{-1} in *E. coli* on the samples compared to those prepared with sodium nitrite. The Ames test confirmed that PAW treatment did not exhibit genotoxicity on the ham (Yong et al., 2018).

5.2 | PAW as thawing medium for frozen meats

The effect of PAW on chicken thawing for microbial inactivation was observed by Qian et al. (2022), showing that the presence of nitric oxide radicals in PAW reduced the bacterial population in the range of 0.62 to 1.17 $\log_{10}$ reduction CFU.g^{-1} and slowed down the lipid oxidation of poultry meats. Liao et al. (2020) revealed that PAW thawing for frozen beef maintained the quality of the beef and posed the highest antimicrobial inactivation, with a reduction in total viable count (TVC) of 1.62 $\log_{10}$ CFU.g^{-1}, compared to microwave thawing (1.41 $\log_{10}$ CFU.g^{-1}) and thawing with slightly acidic electrolyzed water (0.83 $\log_{10}$ CFU.g^{-1}).

5.3 | PAW effects on safety and quality of meats

Table 2 shows different applications of PAW, recently reported in the scientific literature, for the disinfection of fish, chicken, and beef. The extent of the antimicrobial effect of PAW not only relies on the bacterial species, whether the bacteria are Gram-positive or Gram-negative, as discussed in Section 4, but also on its mode of growth and whether the bacterial cells are planktonic or adhered to surfaces. It should be noted that the antimicrobial inactivation of PAW against adhered bacterial cells are typically less efficient than those against planktonic cells (Kamgang-Youbi et al., 2009).

Liu et al. (2021b) compared the inactivation of PAW against *S. putrefaciens* in yellow river carps with water alone, achieving 1.03 $\log_{10}$ reduction CFU g^{-1} at the treatment time of 6 min with no significant difference in the L^* and b^* value of the samples. PAW significantly reduced the pH of yellow river carp from 7.31 to 5.46 due to the acidification of water. The author concluded that the nitrite and nitrate formed in PAW initiated the lipid oxidation of the samples with an increased value in the thiobarbituric acid reactive substances (TBARS) (Liu et al., 2021b).

PAW was also found to maintain the color and texture properties of salmon fillets while resulting 2.04 $\log_{10}$ reduction CFU.g^{-1} against *S. putrefaciens* (Zhu et al., 2023). Chanioti et al. (2023) reported that PAW could extend the shelf life of sea bream fillets by at least 60%. Zhao et al. (2020b) obtained a complete reduction of PAW inactivation (>7 $\log_{10}$ reduction CFU.mL^{-1}) against *P. fluorescens* in mackerel fillets after 24 h of storage time. PAW caused cell shrinkage compared to untreated samples with an intact bacterial surface, which was confirmed by the authors using a scanning electron microscope (SEM).

Jyung et al. (2023) indicated that the combination of PAW and 1% lactic acid can be efficiently applied to mackerel in ice form, which resulted in a 4.53 $\log_{10}$ reduction of PAW-resistant *Listeria monocytogenes* while maintaining the quality of the mackerel. Chaijan et al. (2022) investigated the influence of PAW and whey protein isolated-crude ginger extract coating (WC) for the inhibition of *Pseudomonas* spp. in sea bass steaks during the storage time of up to 30 days at 4°C. After a storage time of 20 days, the TBARS values of PAW-treated samples were about the threshold of TBARS rancidity at 2.00–2.50 mg MDA kg^{-1}, which were mitigated by coating the meat samples with WC after PAW treatment. Compared to untreated samples, PAW-treated samples with and without WC slowed down discoloration (Chaijan et al., 2022).

Liao et al. (2018) investigated the effect of PAW in the form of ice for the microbial safety of shrimps. PAW was first prepared via a DBD and stored at −20°C for 24 h, forming PAW-ice. At the meat storage time of 6 days, the TVC of PAW-treated shrimps reached the value of 4.40 $\log_{10}$ CFU.g^{-1}, below the threshold of meat freshness for shrimps (6.00 $\log_{10}$ CFU.g^{-1}). PAW-ice had a lower TVC at 6.50 $\log_{10}$ CFU.g^{-1} compared to water-ice (8.60 $\log_{10}$ CFU.g^{-1}) at the meat storage time of 9 days, with the ability to (i) retard the lipid oxidation and protein degradation of the meat samples and (ii) reduce the development of melanosis in the shrimp samples. On the other hand, Ke et al. (2023) reported that nitrite in PAW reduced the content of malonaldehyde (MDA) in tuna muscle. Overall, PAW exhibits a remarkable ability to prolong the shelf life of fish and shrimp. However, a more in-depth investigation is required to determine the exact inactivation mechanisms of PAW.

Kang et al. (2019) proved that PAW was effective to inactivate *P. deceptionensis* CM2 adhered on chicken breasts with 1.05 $\log_{10}$ reduction CFU.g^{-1} at the treatment time of 12 min with no impacts on the texture, color, odor, and acceptability of the samples. Mai-Prochnow et al. (2020) investigated the effect of in situ PAW treatment using a plasma-bubble reactor for the inactivation of *P. fluorescens* adhered on chicken skins, achieving 1.40 $\log_{10}$ reduction CFU.mL^{-1} at the treatment time of 15 min. The generated nitrate, ozone, hydroxyl, and peroxide in the liquid were reported to influence the antimicrobial inactivation without visible changes in the chicken samples (Mai-Prochnow et al., 2020). Grosse-Peclum et al. (2023) reported that PAW

15414337, 0, Downloaded from https://ift.onlinelibrary.wiley.com/doi/10.1111/1541-4337.13250 by CochraneArgentina, Wiley Online Library on [13/10/2023]. See the Terms and Conditions (https://onlinelibrary.wiley.com/terms-and-conditions) on Wiley Online Library for rules of use; OA articles are governed by the applicable Creative Commons License

TABLE 2 Recent applications of plasma-activated water for inactivation of meat products.

Type of meat products	Generation of PAW			Microbial inactivation			
	Volume	Plasma device, working gas, power	Plasma activation time	Microorganism	Treatment time	Reduction	Reference
Yellow river carp fillet	200 mL	Plasma jet, air, 750 W	120 s	*Shewanella putrefaciens*	6 min	1.03-$\log_{10}$ CFU.g^{-1}	Liu et al. (2021b)
Atlantic salmon fillet	Not given	Plasma jet, 320 W	5 min	*Shewanella putrefaciens*	120 s	2-$\log_{10}$ CFU.mL^{-1}	Zhu et al. (2023)
Seam bream fillet	20 mL	Plasma jet, helium, 82 kHz, 7.2 kV	16 min	Total aerobic bacteria	20 min	<2.00-$\log_{10}$ CFU.g^{-1}	Chanioti et al. (2023)
Fresh mackerel fillet	30 mL	Plasma jet, air	15 min	*Pseudomonas fluorescens*	24 h	>7.00-$\log_{10}$ CFU.mL^{-1}	Zhao et al. (2020b)
Mackerel	300 mL	DBD, air, 4.5 kV, 20 kHz	120 min	*Listeria monocytogenes*	10 min	4.53-$\log_{10}$ CFU.mL^{-1}	Jyung et al. (2023)
Sea bass steak	Not given	Radio frequency, air, 28 W	120 s	*Pseudomonas* spp.	Up to 30 days at 4^{0}C	Not given	Chaijan et al. (2022)
Silver pomfret	500 mL	Dielectric barrier discharge, air, 1.95 A, 70 V	8 min	Total viable count	5 min	0.53-$\log_{10}$ CFU.g^{-1}	Esua et al. (2022)
Fresh shrimp	100 mL	Dielectric barrier discharge, air, 30 W	10 min	Total viable count	9 days	2.1-$\log_{10}$ CFU.g^{-1}	Liao et al. (2018)
Fresh chicken breast	200 mL	Gliding arc discharge, air, 750 W	30–90 s	*Pseudomonas deceptionensis* CM2	12 min	1.05-$\log_{10}$ CFU.g^{-1}	Kang et al. (2019)
Chicken skin	80 mL	Plasma-bubble discharge, air, 2.5 to 9.4 W	5–15 min	*Pseudomonas fluorescens*	15 min	1.40-$\log_{10}$ CFU.mL^{-1}	Mai-Prochnow et al. (2020)
Cooked chicken breast	100 mL	Dielectric barrier discharge, air, 42 W	20 min	*Staphylococcus aureus*	20 min	2.09- to 2.29-$\log_{10}$ CFU.g^{-1}	Wang et al. (2021)
Fresh chicken carcass	300 mL	An array of 10 plasma tubes, 17 kHz, 16.6 kV, 400 W	20 min	*Escherichia coli*, *Campylobacter. jejuni*	1 min	5.12-$\log_{10}$ CFU.mL^{-1}, 4.20-$\log_{10}$ CFU.mL^{-1}	Grosse-Peclum et al. (2023)

(Continues)

15414337, 0, Downloaded from https://ift.onlinelibrary.wiley.com/doi/10.1111/1541-4337.13250 by CochraneArgentina, Wiley Online Library on [13/10/2023]. See the Terms and Conditions (https://onlinelibrary.wiley.com/terms-and-conditions) on Wiley Online Library for rules of use; OA articles are governed by the applicable Creative Commons License

TABLE 2 (Continued)

Type of meat products	Generation of PAW			Microbial inactivation			
	Volume	Plasma device, working gas, power	Plasma activation time	Microorganism	Treatment time	Reduction	Reference
Fresh chicken meat and skin	20 mL	Plasma jet, argon	6.5 min	*Escherichia coli*, *Staphylococcus aureus*	60 min	0.46-$\log_{10}$ CFU.mL^{-1}, 0.33-$\log_{10}$ CFU.mL^{-1}	Royintarat et al. (2020)
Fresh beef	40 mL	Microplasma array, air	30 min	Surface microorganisms	24 days	2.00-$\log_{10}$ CFU.g^{-1}	Zhao et al. (2020c)
Fresh beef	160 mL	Plasma jet, He + 0.2% N_2 and He + 0.2% O_2	2–10 min	Total aerobic bacteria	20 days at 5^{0}C	>0.80-$\log_{10}$ CFU.g^{-1}	Lotfy and Khalil (2022)
Fresh beef	200 mL	Pin-to-liquid discharge, 60 kHz	30 min	Planktonic *Escherichia coli*, planktonic *Salmonella* Typhimurium	300 s, 240 s	4.00-$\log_{10}$ CFU.mL^{-1}, 5.90-$\log_{10}$ CFU.mL^{-1}	Astorga et al. (2022)
Fresh beef	1500 mL	Hybrid plasma discharge, air, 60 kHz, 45.1 W	30 min	*Salmonella* Typhimurium	15, 30, 60 s	0.696-$\log_{10}$ CFU.mL^{-1}	Hadinoto, et al. (2023)
Beef extract	200 mL	Plasma jet, air	60 s	*Escherichia coli*, *Staphylococcus aureus*	15 min	1.46- to 2.33-$\log_{10}$ CFU.mL^{-1}, 0.78- to 1.50-$\log_{10}$ CFU.mL^{-1}	Xiang et al. (2019)

15414337, 0, Downloaded from https://ift.onlinelibrary.wiley.com/doi/10.1111/1541-4337.13250 by CochraneArgentina, Wiley Online Library on [13/10/2023]. See the Terms and Conditions (https://onlinelibrary.wiley.com/terms-and-conditions) on Wiley Online Library for rules of use; OA articles are governed by the applicable Creative Commons License

caused slight differences in pH, color, and myoglobin redox forms when it interacted with chicken carcass, but these differences were not perceived during the sensory analysis.

Wang et al. (2021) evaluated that PAW produced by DBD did not impact the surface color of the cooked chickens. Rising the activation time of PAW from 5 to 20 min increased the inactivation efficiency against *S. aureus* adherent on the chicken samples due to the RONS in PAW interacting with the bacterial cells. As a result, 2.09 to 2.29 $\log_{10}$ reduction CFU.g^{-1} was achieved with PAW prepared at 20 min. Royintarat et al. (2020) showed that 0.46 and 0.33 $\log_{10}$ reduction CFU.mL^{-1} were achieved for the inactivation of PAW against *E. coli* and *S. aureus*, respectively, on the surfaces of chicken samples at a treatment time of 60 min. These inactivation efficiencies were attributed to the ROS, such as hydrogen peroxide and hydroxyl, in PAW produced by a plasma jet with argon as the working gas (Royintarat et al., 2020). The authors also reported that PAW-treated chicken samples were comparable to untreated samples in terms of hardness, lipid, and protein.

Zhao et al. (2020c) demonstrated the use of PAW for the preservation of fresh beef with 4.08 $\log_{10}$ CFU.g^{-1} compared to the control samples (6.08 $\log_{10}$ CFU.g^{-1}) after storing the meat samples for 13 days. The preservation effects were associated with the long-lived species in PAW and its low pH. The authors revealed that increasing the storage time at 4°C could improve the antimicrobial inactivation of PAW without causing any negative effects on the pH, total volatile basic nitrogen (TVB-N), TBARS, texture, and color of the beef samples.

Astorga et al. (2022) showed that adding NaCl to the liquid prior to plasma discharge to produce PAW resulted in 5.90 $\log_{10}$ reduction CFU.mL^{-1} in planktonic *S.* Typhimurium (at 240 s of treatment time) and 4.00 $\log_{10}$ reduction CFU.mL^{-1} in planktonic *E. coli* (at 300 s of treatment time). The generated PAW had insignificant changes in the vitamin B6, minerals, protein, pH, L^* values, and b^* values of beef rumps but improved the water holding capacity compared to the untreated samples (Astorga et al., 2022). Interestingly, PAW reduced the a^* values of beef rumps compared to those treated with water and had no significant difference with those treated with lactic acid.

Hadinoto et al. (2023) evaluated the effectiveness of two beef washing methods, such as spraying and immersion, using both PAW and water at contact times of 15, 30, and 60 s. The study found no significant difference between the two methods. In addition, the authors discovered that spraying PAW on beef samples maintained the lightness and hue angle values, TBARS value, water holding capacity, and pH of the samples. However, PAW caused a decrease in the redness, yellowness, and chroma values with a 44.1% reduction in oxymyoglobin values, resulting in meat discoloration on the surface of PAW-treated samples, as shown in Figure 10. The discoloration was mitigated when additional water washing was introduced. Moreover, PAW spraying with and without additional water washing achieved 0.696 and 0.656 $\log_{10}$ reduction CFU.mL^{-1} in *S.* Typhimurium at a 30 s contact time.

Lotfy and Khalil (2022) froze beef samples at −24°C for 24 h, soaked the samples in PAW until the temperature of the meat reached 0°C, and stored them at 5°C for 20 h. The total aerobic bacteria count of beef decreased from 3.10 $\log_{10}$ CFU.g^{-1} (untreated beef) to 0.20 $\log_{10}$ CFU.g^{-1} with PAW generated at the activation time of 10 min, due to the generated reactive species. PAW did not change the TVB-N and L^* value of beef in that study but the activation time of PAW significantly influenced the a^* value (Lotfy & Khalil, 2022). The authors also determined that all the PAW-treated samples (0.28–0.72 mgMDA.kg^{-1}) were still within the acceptable range for consumers, below the threshold rancidity of 1.00 mg MDA.kg^{-1}. However, the authors used pure gases, such as helium, to generate PAW.

Xiang et al. (2019) looked into the inactivation efficiency of PAW against *E. coli* and *S. aureus* in the presence of beef extract at concentrations of 0. 0.5, 1.0. 2.5, and 5.0 mg.L^{-1}. It was discovered that the inactivation of PAW with beef extract against *E. coli* (1.46 to 2.33 $\log_{10}$ reduction CFU.mL^{-1}) and *S. aureus* (0.78 to 1.50 $\log_{10}$ reduction CFU.mL^{-1}) were lower than those without beef extract (3.70 $\log_{10}$ reduction CFU.mL^{-1} for *E. coli* and 2.32 $\log_{10}$ reduction CFU.mL^{-1} for *S. aureus*).

6 | COMBINATION OF PAW WITH ULTRASOUND, MILD HEATING, AND NON-THERMAL PLASMA

Some researchers have combined PAW with other food processing technologies such as ultrasound, mild heating, and NTPs to enhance the antimicrobial activity of PAW. Sysolyatina et al. (2020) produced PAW mist (PAWM) using an ultrasound mist maker, achieving effective bacterial inactivation against planktonic *S.* Typhimurium (decreased by a factor of 166), *L. monocytogenes* (decreased by a factor of 35.5), and *E. coli* (decreased by a factor of 266) in 15 s. Xiang et al. (2019) showed that mild heating during a 4-min contact time with PAW at 40, 50, and 60°C resulted in inactivation values of 0.08, 0.75, and 1.78 $\log_{10}$ reduction CFU.mL^{-1} against *E. coli*, respectively, which were higher than at 25°C. Bai et al. (2020) stated that increasing the temperature of PAW up to 55°C intensified the leakage of the intracellular elements of *Bacillus cereus* cells, reaching a 2.96 $\log_{10}$ reduction CFU.mL^{-1} at the treatment time of 60 min.

Xu et al. (2023) combined NTP and PAW for the inactivation of *S*accharomyces *cerevisiae* and *Aspergillus flavus* by soaking the bacterial cells in PAW after the NTP

15414337, 0, Downloaded from https://ift.onlinelibrary.wiley.com/doi/10.1111/1541-4337.13250 by CochraneArgentina, Wiley Online Library on [13/10/2023]. See the Terms and Conditions (https://onlinelibrary.wiley.com/terms-and-conditions) on Wiley Online Library for rules of use; OA articles are governed by the applicable Creative Commons License

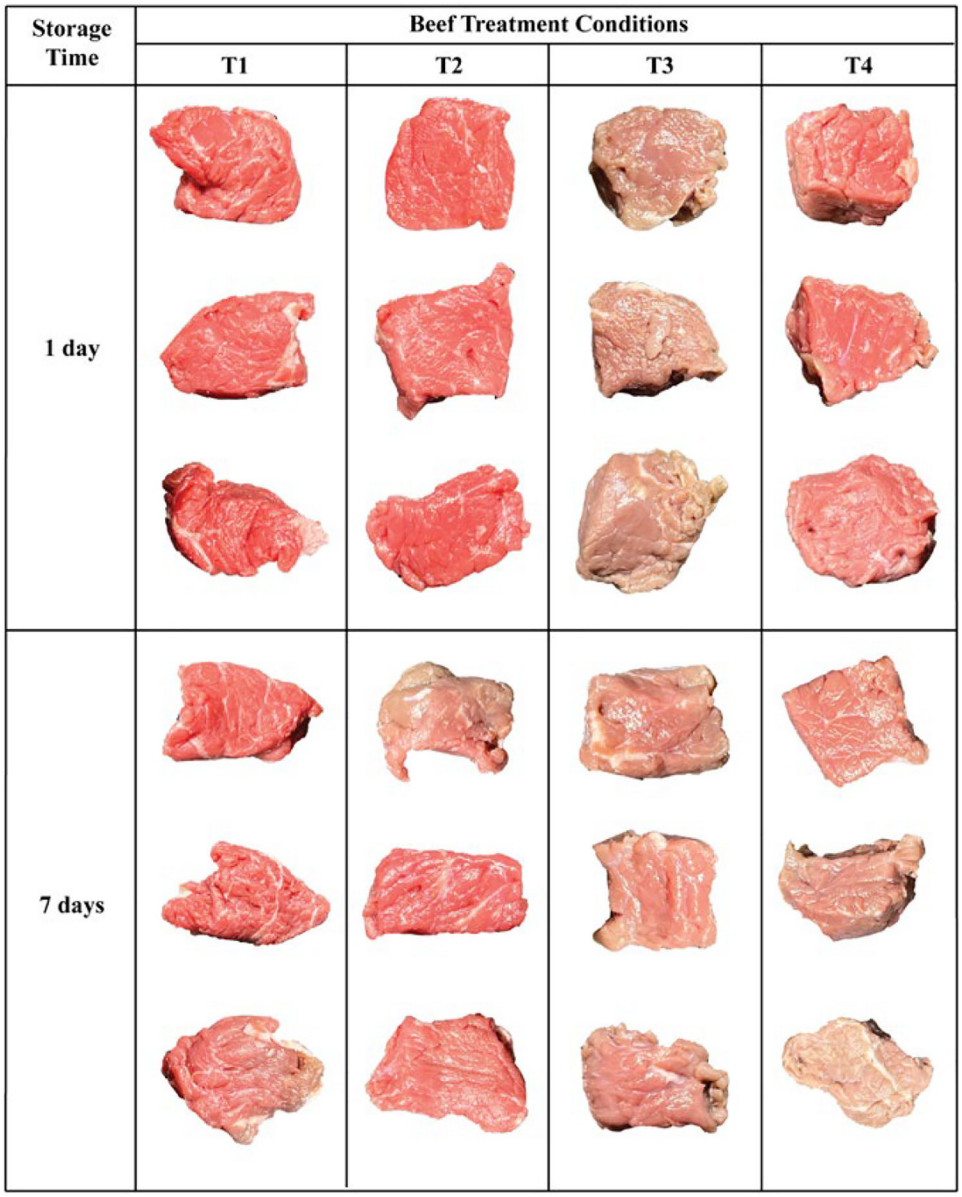

FIGURE 10 Photographs of untreated beef (T1, control) and beef surface samples treated with the water spraying method at 55°C for 30 s (T2), the plasma-activated water (PAW) spraying method at 55°C for 30 s (T3), and the PAW spraying method at 55°C for 30 s followed by the additional water spraying method at 25°C for 60 s (T4) at the meat storage times of 1 day and 7 days at 4°C. Reproduced from Hadinoto et al. (2023) with the permission of Elsevier.

treatment. The SEM photographs revealed that the combined treatment of NTP and PAW changed the surface morphology of the *A. flavus* cells while PAW alone did not (Xu et al., 2023). This combined treatment was attributed to the intracellular superoxide anion and peroxynitrite, inducing oxidative damage to mitochondria, cellular proteins, lipids, and nucleic acids (Xu et al., 2023).

For meats, Royintarat et al. (2020) studied the use of ultrasound to improve the microbial inactivation of PAW as shown in Figure 11. The authors indicated that the ultrasound process increased the penetration rate of PAW and the intracellular ROS while causing no impact on the protein content, lipid content, hardness, and color the chicken samples. Zhao et al. (2021) investigated the combination effect of plasma-activated peracetic acid (PA-PAA), shown in Figure 12, and ultrasound for the microbial safety of mackerels. PA-PAA was reported to increase the reduction of *E. coli* by 0.53 $\log_{10}$ reduction CFU.g^{-1} at a treatment time of 10 min (Zhao et al., 2021). The addition of ultrasound further increased the inactivation to 0.61 $\log_{10}$ reduction CFU.g^{-1}. However, there was no significant differences between PA-PAA with and without ultrasound for the inactivation of adhered *L. innocua* and *P. fluorescens* cells.

15414337, 0, Downloaded from https://ift.onlinelibrary.wiley.com/doi/10.1111/1541-4337.13250 by CochraneArgentina, Wiley Online Library on [13/10/2023]. See the Terms and Conditions (https://onlinelibrary.wiley.com/terms-and-conditions) on Wiley Online Library for rules of use; OA articles are governed by the applicable Creative Commons License

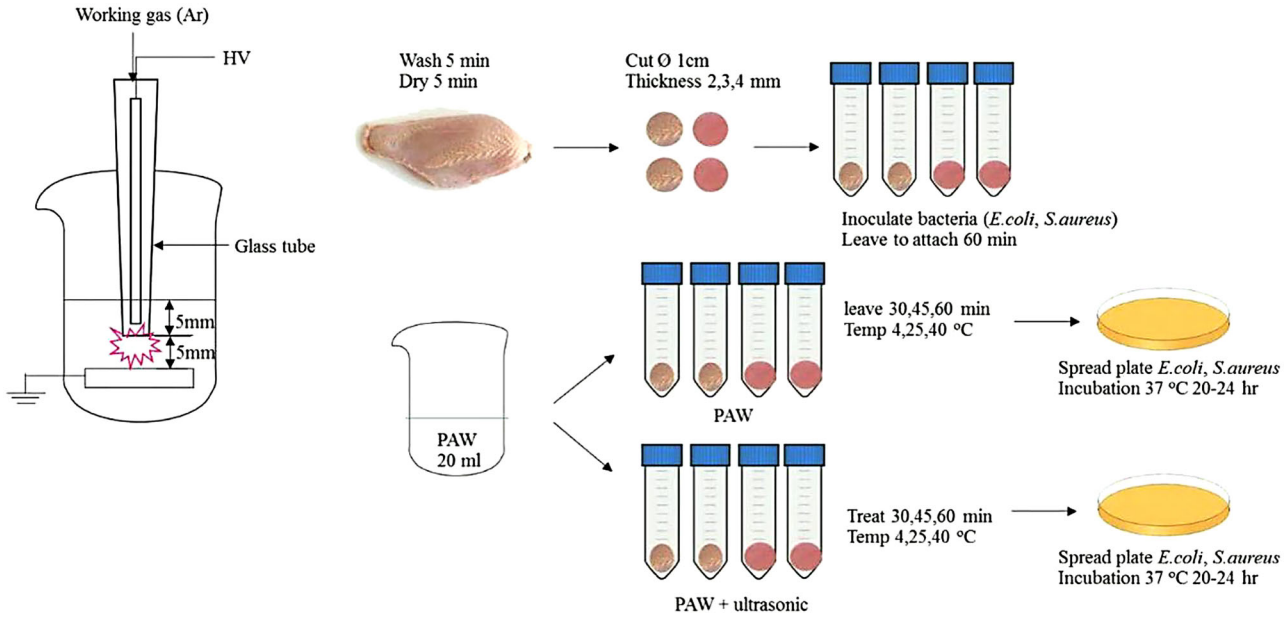

FIGURE 11 Schematic diagram of plasma-activated water (PAW) and PAW-ultrasound treated chicken sample. Reproduced from Royintarat et al. (2020) with the permission of Springer Nature.

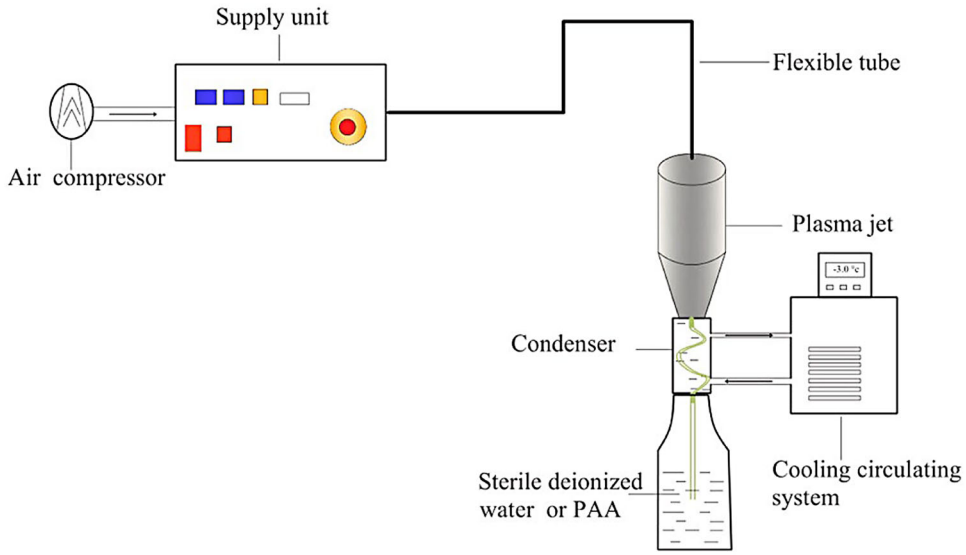

FIGURE 12 Schematic diagram of the plasma device and plasma treatment to peracetic acid. Reproduced from Zhao et al. (2021) with the permission of Elsevier.

7 | CURRENT LIMITATIONS AND FUTURE OPPORTUNITIES

To validate the potential of PAW as an eco-friendly and cost-effective sanitizing process, actual data for environmental impact and cost efficacy is needed, which can be approached with total cost accounting and real-world economic modeling.

The complexity of PAW chemistry remains a challenge to be addressed. The specific effects and mechanism of the microbial inactivation process for the various RONS formed in PAW have not been fully elucidated. The chemistry of PAW is affected by different factors such as the gas composition and the plasma discharge configuration, as explained in Section 2, consequently affecting the antimicrobial capacity of PAW. This is because different discharge configurations alter the composition of RONS in the liquid, and consequently, modulate the energy efficiency and the inactivation activity of PAW.

Large-scale PAW application for meat safety has not yet been implemented. Thus far, considerable efforts have been made in recent years, summarized in Table 1, utilizing

15414337, 0, Downloaded from https://ift.onlinelibrary.wiley.com/doi/10.1111/1541-4337.13250 by CochraneArgentina, Wiley Online Library on [13/10/2023]. See the Terms and Conditions (https://onlinelibrary.wiley.com/terms-and-conditions) on Wiley Online Library for rules of use; OA articles are governed by the applicable Creative Commons License

plasma jet, arc discharge, and DBD for PAW production at a micro-scale and a laboratory scale, which demonstrated (i) the potential of PAW as a greener alternative to traditional chemical disinfectants and (ii) the antimicrobial capacity of PAW with bacterial inactivation ranging from 2.50 to more than 6 $\log_{10}$ reduction CFU.mL^{-1}. However, the reported studies still hinder the practical applications of PAW in the food and agriculture industry, especially the meat industry, due to (i) the production of PAW in low liquid volumes of 5−2000 mL, (ii) the use of high power of up to 750 W to initiate and sustain the discharge, and (iii) the long PAW-food contact time to achieve inactivation, from minutes to hours. As such, issues of cost, efficiency, safety, and productivity must be considered for the implementation of PAW for larger-scale operations.

Different modes of air plasma discharge and water composition have been evaluated to optimize the production of RONS in the liquid, energy efficiency, and inactivation efficacy for food safety (Hadinoto et al., 2021; Rothwell et al., 2022). Efforts have been made to produce PAW in more commercially relevant volumes, notably by Hadinoto, Rao, et al. (2023) and Hadinoto, Yang, et al. (2023) who have achieved production volumes of a few liters. However, the actual implementation of PAW in a scale required for the meat industry has not yet been accomplished.

Another point that needs to be considered is the type of water used during the generation of PAW for meat safety. Several authors generated PAW with distilled or MilliQ$^{\text{Å}}$ water. Increasing the initial conductivity of water prior to plasma discharge also influences the composition of RONS in the solution because of the increased plasma density with the increased electric field at higher initial conductivity (Lu et al., 2012).

Hadinoto et al. (2023) demonstrated the ability of PAW spraying (with the additional of 8 mM NaCl prior to plasma discharge to inactivate *S*. Typhimurium on beef samples, which was found to be higher than water spraying in the contact time of 30 s. In terms of the meat quality, PAW maintained the lightness and hue angle values, TBARS value, water holding capacity, and pH of the beef samples, but decreased their redness, yellowness, chroma, and oxymyoglobin values. These decreased values were mitigated by introducing an additional water washing, displaying no color differences (ΔE), as detected by human eyes, compared to water-treated samples. Further research is required to develop strategies to maintain the redness of red meat compared to washing with water only.

Studies on bacterial resistance are also required because (i) bacteria become more tolerant to some stresses due to a particular stress effect and (ii) different types of stress reactions in bacteria affect the inactivation process and complicate the PAW application. Moreover, the inactivation effectiveness of PAW as a function of the initial microbial population should be investigated. These will complement the microbiological studies toward the commercialization of PAW technology.

Toxicology research is essential to fulfilling regulatory requirements. Considering different market policies and food standard guidelines is important for the adoption of this technology in the meat industry. Moreover, a key factor for the industry adoption of PAW is consumer buying interest. The acceptability of PAW-treated meat by consumers is an important determinant for government decision-making. Assessing the health, economic, social, and environmental risks and benefits perceived by consumers should be investigated. In the near future, regulatory agencies will need to establish regulations and conduct risk assessments to accommodate PAW's increasing industrial and commercial potential.

8 | CONCLUSIONS

The disinfectant capacity of PAW against foodborne microorganisms for the decontamination of meats and meat products has been reported in the literature. In this review, common generations of PAW and its physiochemical properties were discussed. Among several PAW generation methods, the use of multiphase discharge via plasma bubbles needs further study as it may increase the energy efficiency during plasma discharge, enhancing the PAW production efficiency, due to the larger liquid–gas interfacial area around the bubbles that reduce the mass transfer limitations on the gas–liquid interface increasing the production and dissolution of NO_3^- and O_3, as explained in Section 2. The reaction pathways associated with the generation of short-lived and long-lived RONS in PAW were also outlined.

PAW possesses a remarkable ability for bacterial inactivation under various feeding gases, such as argon, oxygen, and nitrogen, that involves different reaction pathways to produce the gaseous excited species during the discharge. These gases can induce the formation of certain RONS in PAW affecting its bacterial inactivation. This review highlighted current studies on PAW inactivation against various planktonic bacteria and the inactivation mechanism of PAW. The optimization of critical processing parameters to improve the PAW inactivation, such as gas type, gas flow rate, storage time, storage temperature, water type, and liquid temperature, were discussed. The promising performance and applications of PAW for meat curing, thawing frozen meats and meat decontamination were reviewed. Recent reports on the ultrasound process, mild heating, and NTP combined with PAW to improve the inactivation efficacy of PAW were reviewed. This review identified the need to develop energy-efficient systems for

15414337, 0, Downloaded from https://ift.onlinelibrary.wiley.com/doi/10.1111/1541-4337.13250 by CochraneArgentina, Wiley Online Library on [13/10/2023]. See the Terms and Conditions (https://onlinelibrary.wiley.com/terms-and-conditions) on Wiley Online Library for rules of use; OA articles are governed by the applicable Creative Commons License

the commercial-scale production of PAW aiming for its potential application as a meat disinfectant, especially for beef, without affecting the meat quality.

AUTHOR CONTRIBUTIONS

Koentadi Hadinoto: Conceptualization; writing—original draft; writing—review and editing; visualization. **Brendan A. Niemira**: Writing—review and editing. **Francisco J. Trujillo**: Supervision; project administration; writing—review and editing; conceptualization; funding acquisition.

ACKNOWLEDGMENTS

This work was supported by the Australian Meat Processor Corporation (AMPC) [Project Code 2016-1326]. The authors are grateful to Drs. C. Bardsley and M. Olanya for their reviews of this manuscript. Mention of trade names or commercial products in this article is solely for the purpose of providing specific information and does not imply recommendation or endorsement by the U.S. Department of Agriculture. USDA is an equal opportunity provider and employer.

Open access publishing facilitated by University of New South Wales, as part of the Wiley - University of New South Wales agreement via the Council of Australian University Librarians.

CONFLICT OF INTEREST STATEMENT

The authors declare no conflicts of interest.

ORCID

Koentadi Hadinoto https://orcid.org/0000-0002-2433-0755
Brendan A. Niemira https://orcid.org/0000-0001-9472-1025
Francisco J. Trujillo https://orcid.org/0000-0002-0652-6164

REFERENCES

Akiyama, H., & Akiyama, M. (2020). Pulsed discharge plasmas in contact with water and their applications. *IEEJ Transactions on Electrical and Electronic Engineering*, *16*(1), 6–14. https://doi.org/10.1002/tee.23282

Ali, M., Cheng, J.-H., & Sun, D.-W. (2021). Effect of plasma activated water and buffer solution on fungicide degradation from tomato (*Solanum lycopersicum*) fruit. *Food Chemistry*, *350*, 129195. https://doi.org/10.1016/j.foodchem.2021.129195

Anuntagool, J., Srangsomjit, N., Thaweewong, P., & Alvarez, G. (2023). A review on dielectric barrier discharge nonthermal plasma generation, factors affecting reactive species, and microbial inactivation. *Food Control*, *153*, 109913. https://doi.org/10.1016/j.foodcont.2023.109913

Asimakopoulou, E., Ekonomou, S. I., Papakonstantinou, P., Doran, O., & Stratakos, A. C. (2022). Inhibition of corrosion causing *Pseudomonas aeruginosa* using plasma-activated water. *Journal of Applied Microbiology*, *132*(4), 2781–2794. https://doi.org/10.1111/jam.15391

Astorga, J. B., Hadinoto, K., Cullen, P., Prescott, S., & Trujillo, F. J. (2022). Effect of plasma activated water on the nutritional composition, storage quality and microbial safety of beef. *LWT*, *154*, 112794. https://doi.org/10.1016/j.lwt.2021.112794

Baek, K. H., Yong, H. I., Yoo, J. H., Kim, J. W., Byeon, Y. S., Lim, J., Yoon, S. Y., Ryu, S., & Jo, C. (2020). Antimicrobial effects and mechanism of plasma activated fine droplets produced from arc discharge plasma on planktonic *Listeria monocytogenes* and *Escherichia coli* O157:H7. *Journal of Physics D: Applied Physics*, *53*(12), 124002. https://doi.org/10.1088/1361-6463/ab634d

Bai, Y., Muhammad, A. I., Hu, Y., Koseki, S., Liao, X., Chen, S., Ye, X., Liu, D., & Ding, T. (2020). Inactivation kinetics of *Bacillus cereus* spores by plasma activated water (PAW). *Food Research International*, *131*, 109041. https://doi.org/10.1016/j.foodres.2020.109041

Bălan, G. G., Roșca, I., Ursu, E.-L., Doroftei, F., Bostănaru, A.-C., Hnatiuc, E., Năstasă, V., Șandru, V., Ștefănescu, G., Trifan, A., & Mareș, M. (2018). Plasma-activated water: A new and effective alternative for duodenoscope reprocessing. *Infection and Drug Resistance*, *11*, 727–733. https://doi.org/10.2147/IDR.S159243

Beckman, J. S., Beckman, T. W., Chen, J., Marshall, P. A., & Freeman, B. A. (1990). Apparent hydroxyl radical production by peroxynitrite: Implications for endothelial injury from nitric oxide and superoxide. *Proceedings of the National Academy of Sciences of the United States of America*, *87*(4), 1620–1624. https://doi.org/10.1073/pnas.87.4.1620

Bolouki, N., Kuan, W.-H., Huang, Y.-Y., & Hsieh, J.-H. (2021). Characterizations of a plasma-water system generated by repetitive microsecond pulsed discharge with air, nitrogen, oxygen, and argon gases species. *Applied Sciences*, *11*(13), 6158. https://doi.org/10.3390/app11136158

Brandenburg, R. (2017). Dielectric barrier discharges: Progress on plasma sources and on the understanding of regimes and single filaments. *Plasma Sources Science and Technology*, *26*(5), 053001. https://doi.org/10.1088/1361-6595/aa6426

Chaijan, M., Chaijan, S., Panya, A., Nisoa, M., Cheong, L.-Z., & Panpipat, W. (2022). Combined effects of prior plasma-activated water soaking and whey protein isolate-ginger extract coating on the cold storage stability of Asian sea bass (*Lates calcarifer*) steak. *Food Control*, *135*, 108787. https://doi.org/10.1016/j.foodcont.2021.108787

Chanioti, S., Giannoglou, M., Stergiou, P., Passaras, D., Dimitrakellis, P., Kokkoris, G., Gogolides, E., & Katsaros, G. (2023). Plasma-activated water for disinfection and quality retention of sea bream fillets: Kinetic evaluation and process optimization. *Innovative Food Science & Emerging Technologies*, *85*, 103334. https://doi.org/10.1016/j.ifset.2023.103334

Chiozzi, V., Agriopoulou, S., & Varzakas, T. (2022). Advances, applications, and comparison of thermal (pasteurization, sterilization, and aseptic packaging) against non-thermal (ultrasounds, UV radiation, ozonation, high hydrostatic pressure) technologies in food processing. *Applied Sciences*, *12*(4), 2202. https://doi.org/10.3390/app12042202

15414337, 0, Downloaded from https://ift.onlinelibrary.wiley.com/doi/10.1111/1541-4337.13250 by CochraneArgentina, Wiley Online Library on [13/10/2023]. See the Terms and Conditions (https://onlinelibrary.wiley.com/terms-and-conditions) on Wiley Online Library for rules of use; OA articles are governed by the applicable Creative Commons License

Cho, C., Jin, Y.-S., Shon, C.-H., & Kim, D. (2023). Plasma activated water production by magnetically driven gliding arc. *IEEE Transactions on Plasma Science*, 1–7. https://doi.org/10.1109/tps.2023.3290555

Cubas, A. L. V., Ferreira, F. M., Gonçalves, D. B., Machado, M. D. M., Debacher, N. A., & Moecke, E. H. S. (2021). Influence of non-thermal plasma reactor geometry and plasma gas on the inactivation of Escherichia coli in water. *Chemosphere*, *277*, 130255. https://doi.org/10.1016/j.chemosphere.2021.130255

Degala, H. L., Mahapatra, A. K., Demirci, A., & Kannan, G. (2018). Evaluation of non-thermal hurdle technology for ultraviolet-light to inactivate *Escherichia coli* K12 on goat meat surfaces. *Food Control*, *90*, 113–120. https://doi.org/10.1016/j.foodcont.2018.02.042

Domínguez, R., Pateiro, M., Gagaoua, M., Barba, F. J., Zhang, W., & Lorenzo, J. M. (2019). A comprehensive review on lipid oxidation in meat and meat products. *Antioxidants*, *8*(10), 429. https://doi.org/10.3390/antiox8100429

Du, C. M., Wang, J., Zhang, L., Li, H. X., Liu, H., & Xiong, Y. (2012). The application of a non-thermal plasma generated by gas–liquid gliding arc discharge in sterilization. *New Journal of Physics*, *14*(1), 013010. https://doi.org/10.1088/1367-2630/14/1/013010

Gan, Z., Zhang, Y., Gao, W., Wang, S., Liu, Y., Xiao, Y., Zhuang, X., Sun, A., & Wang, R. (2022). Effects of nonthermal plasma-activated water on the microbial sterilization and storage quality of blueberry. *Food Bioscience*, *49*, 101857. https://doi.org/10.1016/j.fbio.2022.101857

Gao, Y., Li, M., Sun, C., & Zhang, X. (2022). Microbubble-enhanced water activation by cold plasma. *Chemical Engineering Journal*, *446*, 137318. https://doi.org/10.1016/j.cej.2022.137318

Ghimire, B., Szili, E. J., Patenall, B. L., Lamichhane, P., Gaur, N., Robson, A. J., Trivedi, D., Thet, N. T., Jenkins, A. T. A., Choi, E. H., & Short, R. D. (2021). Enhancement of hydrogen peroxide production from an atmospheric pressure argon plasma jet and implications to the antibacterial activity of plasma activated water. *Plasma Sources Science and Technology*, *30*(3), 035009. https://doi.org/10.1088/1361-6595/abe0c9

Giller, K. E., Delaune, T., Silva, J. V., Descheemaeker, K., van de ven, G., Schut, A. G. T., van Wijk, M., Hammond, J., Hochman, Z., Taulya, G., Chikowo, R., Narayanan, S., Kishore, A., Bresciani, F., Teixeira, H. M., Andersson, J. A., & van Ittersum, M. K. (2021). The future of farming: Who will produce our food? *Food Security*, *13*(5), 1073–1099. https://doi.org/10.1007/s12571-021-01184-6

Große-Peclum, V., Siekmann, L., Krischek, C., Avramidis, G., Ochs, C., Viöl, W., & Plötz, M. (2023). Using TRIS-buffered plasma-activated water to reduce pathogenic microorganisms on poultry carcasses with evaluation of physicochemical and sensory parameters. *Foods*, *12*(5), 1113. https://doi.org/10.3390/foods12051113

Guo, J., Wang, J., Xie, H., Jiang, J., Li, C., Li, W., Li, L., Liu, X., & Lin, F. (2022). Inactivation effects of plasma-activated water on *Fusarium graminearum*. *Food Control*, *134*, 108683. https://doi.org/10.1016/j.foodcont.2021.108683

Guo, L., Zhao, P., Yao, Z., Li, T., Zhu, M., Wang, Z., Huang, L., Niyazi, G., Liu, D., & Rong, M. (2023). Inactivation of Salmonella enteritidis on the surface of eggs by air activated with gliding arc discharge plasma. *Food Control*, *148*, 109662. https://doi.org/10.1016/j.foodcont.2023.109662

Guragain, R. P., Baniya, H. B., Shrestha, B., Guragain, D. P., & Subedi, D. P. (2023). Improvements in germination and growth of sprouts irrigated using plasma activated water (PAW). *Water*, *15*(4), 744. https://doi.org/10.3390/w15040744

Hadinoto, K., Astorga, J. B., Masood, H., Zhou, R., Alam, D., Cullen, P. J., Prescott, S., & Trujillo, F. J. (2021). Efficacy optimization of plasma-activated water for food sanitization through two reactor design configurations. *Innovative Food Science & Emerging Technologies*, *74*, 109381. https://doi.org/10.1016/j.ifset.2021.102867

Hadinoto, K., Rao, N. R. H., Astorga, J. B., Zhou, R., Biazik, J., Zhang, T., Masood, H., Cullen, P. J., Prescott, S., Henderson, R. K., & Trujillo, F. J. (2023). Hybrid plasma discharges for energy-efficient production of plasma-activated water. *Chemical Engineering Journal*, *451*, 138643. https://doi.org/10.1016/j.cej.2022.138643

Hadinoto, K., Yang, H., Zhang, T., Cullen, P. J., Prescott, S., & Trujillo, F. J. (2023). The antimicrobial effects of mist spraying and immersion on beef samples with plasma-activated water. *Meat Science*, *200*, 109165. https://doi.org/10.1016/j.meatsci.2023.109165

Han, Q.-Y., He, Z.-Y., Zhong, C.-S., Wen, X., & Ni, Y.-Y. (2022). The optimization of plasma activated water (PAW) generation and the inactivation mechanism of PAW on Escherichia coli. *Journal of Food Processing and Preservation*, *46*(11), e17120. https://doi.org/10.1111/jfpp.17120

Han, S., Jo, J. Y., Park, S. R., Choi, C., & Ha, S.-D. (2021). Impact of chlorine dioxide and electron-beam irradiation for the reduction of murine norovirus in low-salted "jogaejeotgal", a traditional Korean salted and fermented clam. *International Journal of Food Microbiology*, *342*, 109073. https://doi.org/10.1016/j.ijfoodmicro.2021.109073

Han, J.-Y., Park, S.-H., & Kang, D.-H. (2023). Effects of plasma bubble-activated water on the inactivation against foodborne pathogens on tomatoes and its wash water. *Food Control*, *144*, 109381. https://doi.org/10.1016/j.foodcont.2022.109381

Herianto, S., Hou, C.-Y., Lin, C.-M., & Chen, H.-L. (2021). Nonthermal plasma-activated water: A comprehensive review of this new tool for enhanced food safety and quality. *Comprehensive Reviews in Food Science and Food Safety*, *20*(1), 583–626. https://doi.org/10.1111/1541-4337.12667

Hong, J., Zhang, T., Zhou, R., Zhou, R., Ostikov, K., Rezaeimotlagh, A., & Cullen, P. J. (2021). Plasma bubbles: A route to sustainable chemistry. *AAPPS Bulletin*, *31*(1), 26. https://doi.org/10.1007/s43673-021-00027-y

Ikawa, S., Tani, A., Nakashima, Y., & Kitano, K. (2016). Physicochemical properties of bactericidal plasma-treated water. *Journal of Physics D: Applied Physics*, *49*(42), 425401. https://doi.org/10.1088/0022-3727/49/42/425401

Inguglia, E. S., Oliveira, M., Burgess, C. M., Kerry, J. P., & Tiwari, B. K. (2020). Plasma-activated water as an alternative nitrite source for the curing of beef jerky: Influence on quality and inactivation of Listeria innocua. *Innovative Food Science & Emerging Technologies*, *59*, 102276. https://doi.org/10.1016/j.ifset.2019.102276

Jadhav, H. B., & Annapure, U. (2021). Consequences of non-thermal cold plasma treatment on meat and dairy lipids—A review. *Future Foods*, *4*, 100095. https://doi.org/10.1016/j.fufo.2021.100095

Jin, Y. S., Cho, C., Kim, D., Sohn, C. H., Ha, C.-S., & Han, S.-T. (2020). Mass production of plasma activated water by an atmospheric pressure plasma. *Japanese Journal of Applied Physics*, *59*, SHHF05. https://doi.org/10.35848/1347-4065/ab7e13

Jyung, S., Kang, J.-W., & Kang, D.-H. (2022). *L. monocytogens* exhibited less cell membrane damage, lipid peroxidation, and

15414337, 0, Downloaded from https://ift.onlinelibrary.wiley.com/doi/10.1111/1541-4337.13250 by CochraneArgentina, Wiley Online Library on [13/10/2023]. See the Terms and Conditions (https://onlinelibrary.wiley.com/terms-and-conditions) on Wiley Online Library for rules of use; OA articles are governed by the applicable Creative Commons License

intracellular reactive oxygen species accumulation after plasma-activated water treatment compared to *E. coli* O157:H7 and S. Typhimurium. *Food Microbiology*, *108*, 104098. https://doi.org/10.1016/j.fm.2022.104098

Jyung, S., Kang, J.-W., & Kang, D.-H. (2023). Inactivation of Listeria monocytogenes through the synergistic interaction between plasma-activated water and organic acid. *Food Research International*, *167*, 112687. https://doi.org/10.1016/j.foodres.2023.112687

Kalogianni, A. I., Lazou, T., Bossis, I., & Gelasakis, A. I. (2020). Natural phenolic compounds for the control of oxidation, bacterial spoilage, and foodborne pathogens in meat. *Foods*, *9*(6), 794. https://doi.org/10.3390/foods9060794

Kamgang-Youbi, G., Herry, J.-M., Meylheuc, T., Brisset, J.-L., Bellon-Fontaine, M.-N., Doubla, A., & Naïtali, M. (2009). Microbial inactivation using plasma-activated water obtained by gliding electric discharges. *Letter in Applied Microbiology*, *48*(1), 13–18. https://doi.org/10.1111/j.1472-765X.2008.02476.x

Kang, C., Xiang, Q., Zhao, D., Wang, W., Niu, L., & Bai, Y. (2019). Inactivation of *Pseudomonas deceptionensis* CM2 on chicken breasts using plasma-activated water. *Journal of Food Science and Technology*, *56*(11), 4938–4945. https://doi.org/10.1007/s13197-019-03964-7

Kasih, T. P., Danil, D., Geraldine, E., & Widyaningrum, D. (2022). Effect of plasma activated water (PAW) in maintaining the quality of cherry tomatoes. *IOP Conference Series: Earth and Environmental Science*, *998*(1), 012063. https://doi.org/10.1088/1755-1315/998/1/012063

Kaushik, N. K., Bhartiya, P., Kaushik, N., Shin, Y., Nguyen, L. N., Park, J. S., Kim, D., & Choi, E. H. (2023). Nitric-oxide enriched plasma-activated water inactivates 229E coronavirus and alters antiviral response genes in human lung host cells. *Bioactive Materials*, *19*, 569–580. https://doi.org/10.1016/j.bioactmat.2022.05.005

Kaushik, N. K., Ghimire, B., Li, Y., Adhikari, M., Veerana, M., Kaushik, N., Jha, N., Adhikari, B., Lee, S.-J., Masur, K., Von Woedtke, T., Weltmann, K.-D., & Choi, E. H. (2018). Biological and medical applications of plasma-activated media, water and solutions. *Biological Chemistry*, *400*(1), 39–62. https://doi.org/10.1515/hsz-2018-0226

Ke, Z., Bai, Y., Yi, Y., Ding, Y., Wang, W., Liu, S., Zhou, X., & Ding, Y. (2023). Why plasma-activated water treatment reduced the malonaldehyde content in muscle foods. *Food Chemistry*, *403*, 134387. https://doi.org/10.1016/j.foodchem.2022.134387

Kim, H., Jung, A. H., Park, S. H., Yoon, Y., & Kim, B. G. (2021). In vitro protein disappearance of raw chicken as dog foods decreased by thermal processing, but was unaffected by non-thermal processing. *Animals*, *11*(5), 1256. https://doi.org/10.3390/ani11051256

Kim, H.-J., Sung, N.-Y., Yong, H. I., Kim, H., Lim, Y., Ko, K. H., Yun, C.-H., & Jo, C. (2016). Mutagenicity and immune toxicity of emulsion-type sausage cured with plasma-treated water. *Korean Journal for Food Science of Animal Resources*, *36*(4), 494–498. https://doi.org/10.5851/kosfa.2016.36.4.494

Kirk, M., Ford, L., Glass, K., & Hall, G. (2014). Foodborne illness, Australia, circa 2000 and circa 2010. *Emerging Infectious Diseases*, *20*(11), 1857–1864. https://doi.org/10.3201/eid2011.131315

Kovačević, V. V., Sretenović, G. B., Obradović, B. M., & Kuraica, M. M. (2022). Low-temperature plasmas in contact with liquids—A review of recent progress and challenges. *Journal of Physics D: Applied Physics*, *55*(47), 473002. https://doi.org/10.1088/1361-6463/ac8a56

Kučerová, K., Machala, Z., & Hensel, K. (2020). Transient spark discharge generated in various N_2/O_2 gas mixtures: Reactive species in the gas and water and their antibacterial effects. *Plasma Chemistry and Plasma Processing*, *40*(3), 749–773. https://doi.org/10.1007/s11090-020-10082-2

Kutasi, K., Bencs, L., Tóth, Z., & Milošević, S. (2022). The role of metals in the deposition of long-lived reactive oxygen and nitrogen species into the plasma-activated liquids. *Plasma Processes and Polymers*, *20*(3), 2200143. https://doi.org/10.1002/ppap.202200143

Lee, H. R., Lee, Y. S., You, Y. S., Huh, J. Y., Kim, K., Hong, Y. C., & Kim, C.-H. (2022). Antimicrobial effects of microwave plasma-activated water with skin protective effect for novel disinfectants in pandemic era. *Scientific Reports*, *12*(1), 5968. https://doi.org/10.1038/s41598-022-10009-1

Liang, J. P., Zhao, Z. L., Zhou, X. F., Yuan, H., Wang, H. L., Wang, W. C., & Yang, D. Z. (2022). The influences of shielding gas and quartz tube on discharge properties and reactive species productions of nanosecond pulsed gas–liquid discharge. *Journal of Physics D: Applied Physics*, *55*(19), 195204. https://doi.org/10.1088/1361-6463/ac4fd5

Liao, X., Su, Y., Liu, D., Chen, S., Hu, Y., Ye, X., Wang, J., & Ding, T. (2018). Application of atmospheric cold plasma-activated water (PAW) ice for preservation of shrimps (*Metapenaeus ensis*). *Food Control*, *94*, 307–314. https://doi.org/10.1016/j.foodcont.2018.07.026

Liao, X., Xiang, Q., Cullen, P. J., Su, Y., Chen, S., Ye, X., Liu, D., & Ding, T. (2020). Plasma-activated water (PAW) and slightly acidic electrolyzed water (SAEW) as beef thawing media for enhancing microbiological safety. *LWT*, *117*, 108649. https://doi.org/10.1016/j.lwt.2019.108649

Lim, J., Hong, E. J., Kim, S. B., & Ryu, S. (2022). The effect of gap distance between a pin and water surface on the inactivation of *Escherichia coli* using a pin-to-water plasma. *International Journal of Moecularl Sciences*, *23*(10), 5423. https://doi.org/10.3390/ijms23105423

Lin, Q., Huang, Y., Li, G., Luo, Z., Wang, L., Li, D., Xiang, Y., Liu, L., Ban, Z., & Li, L. (2023). The journey of prochloraz pesticide in *Citrus sinensis*: Residual distribution, impact on transcriptomic profiling and reduction by plasma-activated water. *Journal of Hazardous Materials*, *448*, 130931. https://doi.org/10.1016/j.jhazmat.2023.130931

Liu, X., Li, Y., Zhang, R., Huangfu, L., Du, G., & Xiang, Q. (2021a). Inactivation effects and mechanisms of plasma-activated water combined with sodium laureth sulfate (SLES) against *Saccharomyces cerevisiae*. *Applied Microbiology and Biotechnology*, *105*(7), 2855–2865. https://doi.org/10.1007/s00253-021-11227-9

Liu, X., Zhang, M., Meng, X., Bai, Y., & Dong, X. (2021b). Effect of plasma-activated water on shewanella putrefaciens population growth and quality of yellow river carp (*Cyprinus carpio*) fillets. *Journal of Food Protection*, *84*(10), 1722–1728. https://doi.org/10.4315/JFP-21-031

Lotfy, K., & Khalil, S. (2022). Effect of plasma-activated water on microbial quality and physicochemical properties of fresh beef. *Open Physics*, *20*(1), 573–586. https://doi.org/10.1515/phys-2022-0049

Lu, P., Boehm, D., Bourke, P., & Cullen, P. J. (2017). Achieving reactive species specificity within plasma-activated water through selective

15414337, 0, Downloaded from https://ift.onlinelibrary.wiley.com/doi/10.1111/1541-4337.13250 by CochraneArgentina, Wiley Online Library on [13/10/2023]. See the Terms and Conditions (https://onlinelibrary.wiley.com/terms-and-conditions) on Wiley Online Library for rules of use; OA articles are governed by the applicable Creative Commons License

generation using air spark and glow discharges. *Plasma Processes and Polymers*, *14*(8), 1600207. https://doi.org/10.1002/ppap.201600207

Lu, N., Li, J., Wu, Y., & Masayuki, S. (2012). Treatment of dye wastewater by using a hybrid gas/liquid pulsed discharge plasma reactor. *Plasma Science and Technology*, *14*(2), 162–166. https://doi.org/10.1088/1009-0630/14/2/15

Ma, R. N., Feng, H. Q., Liang, Y. D., Zhang, Q., Tian, Y., Su, B., Zhang, J., & Fang, J. (2013). An atmospheric-pressure cold plasma leads to apoptosis in *Saccharomyces cerevisiae* by accumulating intracellular reactive oxygen species and calcium. *Journal of Physics D: Applied Physics*, *46*(28), 285401. https://doi.org/10.1088/0022-3727/46/28/285401

Machala, Z., Tarabová, B., Sersenová, D., Janda, M., & Hensel, K. (2019). Chemical and antibacterial effects of plasma activated water: Correlation with gaseous and aqueous reactive oxygen and nitrogen species, plasma sources and air flow conditions. *Journal of Physics D: Applied Physics*, *52*(3), 034002. https://doi.org/10.1088/1361-6463/aae807

Mai-Prochnow, A., Alam, D., Zhou, R., Zhang, T., Ostrikov, K. K., & Cullen, P. J. (2020). Microbial decontamination of chicken using atmospheric plasma bubbles. *Plasma Processes and Polymers*, *18*(1), 2000052. https://doi.org/10.1002/ppap.202000052

Mai-Prochnow, A., Zhou, R., Zhang, T., Ostrikov, K., Mugunthan, S., Rice, S. A., & Cullen, P. J. (2021). Interactions of plasma-activated water with biofilms: Inactivation, dispersal effects and mechanisms of action. *NPJ Biofilms Microbiomes*, *7*(1), 11. https://doi.org/10.1038/s41522-020-00180-6

Man, C., Zhang, C., Fang, H., Zhou, R., Huang, B., Xu, Y., Zhang, X., & Shao, T. (2022). Nanosecond-pulsed microbubble plasma reactor for plasma-activated water generation and bacterial inactivation. *Plasma Processes and Polymers*, *19*(6), 2200004. https://doi.org/10.1002/ppap.202200004

Matra, K., Tanakaran, Y., Luang-In, V., & Theepharaksapan, S. (2022). Enhancement of lettuce growth by PAW spray gliding arc plasma generator. *IEEE Transactions on Plasma Science*, *50*(6), 1430–1439. https://doi.org/10.1109/tps.2021.3105733

Meropoulis, S., & Aggelopoulos, C. A. (2023). Plasma microbubbles vs gas-liquid DBD energized by low-frequency high voltage nanopulses for pollutants degradation in water: Destruction mechanisms, composition of plasma-activated water and energy assessment. *Journal of Environmental Chemical Engineering*, *11*(3), 109855. https://doi.org/10.1016/j.jece.2023.109855

Miller, J. A., & Bowman, C. T. (1989). Mechanism and modeling of nitrogen chemistry in combustion. *Progress in Energy and Combustion Science*, *15*(4), 287–338. https://doi.org/10.1016/0360-1285(89)90017-8

Mir, S. A., Siddiqui, M. W., Dar, B. N., Shah, M. A., Wani, M. H., Roohinejad, S., Annor, G. A., Mallikarjunan, K., Chin, C. F., & Ali, A. (2020). Promising applications of cold plasma for microbial safety, chemical decontamination and quality enhancement in fruits. *Journal of Applied Microbiology*, *129*(3), 474–485. https://doi.org/10.1111/jam.14541

Mogo, J. P. K., Fovo, J. D., Sop-Tamo, B., Mafouasson, H. N. A., Ngwem, M. C. N., Tebu, M. J., Youbi, G. K., & Laminsi, S. (2022). Effect of gliding arc plasma activated water (GAPAW) on maize (*Zea mays* L.) seed germination and growth. *Seeds*, *1*(4), 230–243. https://doi.org/10.3390/seeds1040020

Mohades, S., Lietz, A. M., & Kushner, M. J. (2020). Generation of reactive species in water film dielectric barrier discharges sustained in argon, helium, air, oxygen and nitrogen. *Journal of Physics D: Applied Physics*, *53*(43), 435206. https://doi.org/10.1088/1361-6463/aba21a

Nastasijević, I., Lakićević, B., & Petrović, Z. (2017). Cold chain management in meat storage, distribution and retail: A review. *IOP Conference Series: Earth and Environmental Science*, *85*, 012022. https://doi.org/10.1088/1755-1315/85/1/012022

Neretti, G., Taglioli, M., Colonna, G., & Borghi, C. A. (2016). Characterization of a dielectric barrier discharge in contact with liquid and producing a plasma activated water. *Plasma Sources Science and Technology*, *26*(1), 015013. https://doi.org/10.1088/1361-6595/26/1/015013

Ng, S. W., Slikboer, E., Dickenson, A., Walsh, J. L., Lu, P., Boehm, D., & Bourke, P. (2021). Characterization of an atmospheric pressure air plasma device under different modes of operation and their impact on the liquid chemistry. *Journal of Applied Physics*, *129*(12), 123303. https://doi.org/10.1063/5.0039171

Ning, W., Lai, J., Kruszelnicki, J., Foster, J. E., Dai, D., & Kushner, M. J. (2021). Propagation of positive discharges in an air bubble having an embedded water droplet. *Plasma Sources Science and Technology*, *30*(1), 015005. https://doi.org/10.1088/1361-6595/abc830

Pang, B., Liu, Z., Zhang, H., Wang, S., Gao, Y., Xu, D., Liu, D., & Kong, M. G. (2021). Investigation of the chemical characteristics and anticancer effect of plasma-activated water: The effect of liquid temperature. *Plasma Processes and Polymers*, *19*(1), 2100079. https://doi.org/10.1002/ppap.202100079

Pavlovich, M. J., Ono, T., Galleher, C., Curtis, B., Clark, D. S., Machala, Z., & Graves, D. B. (2014). Air spark-like plasma source for antimicrobial NO_x generation. *Journal of Physics D: Applied Physics*, *47*(50), 505202. https://doi.org/10.1088/0022-3727/47/50/505202

Pawłat, J., Terebun, P., Kwiatkowski, M., Tarabová, B., Kovaľová, Z., Kučerová, K., Machala, Z., Janda, M., & Hensel, K. (2019). Evaluation of oxidative species in gaseous and liquid phase generated by mini-gliding arc discharge. *Plasma Chemistry and Plasma Processing*, *39*(3), 627–642. https://doi.org/10.1007/s11090-019-09974-9

Pereira, P. M. D. C. C., & Vicente, A. F. D. R. B. (2013). Meat nutritional composition and nutritive role in the human diet. *Meat Science*, *93*(3), 586–592. https://doi.org/10.1016/j.meatsci.2012.09.018

Perinban, S., Orsat, V., Gariepy, Y., Lyew, D., & Raghavan, V. (2022). Evaluation of plasma-activated water characteristics and its process optimization. *Journal of Food Process Engineering*, *45*(11), e14156. https://doi.org/10.1111/jfpe.14156

Puertas, E. C., Dzafic, A., & Coulombe, S. (2019). Investigation of the electrode erosion in pin-to-liquid discharges and its influence on reactive oxygen and nitrogen species in plasma-activated water. *Plasma Chemistry and Plasma Processing*, *40*(1), 145–167. https://doi.org/10.1007/s11090-019-10036-3

Qian, J., Wang, C., Zhuang, H., Nasiru, M. M., Zhang, J., & Yan, W. (2021). Evaluation of meat-quality and myofibrillar protein of chicken drumsticks treated with plasma-activated lactic acid as a novel sanitizer. *LWT*, *138*, 110642. https://doi.org/10.1016/j.lwt.2020.110642

15414337, 0, Downloaded from https://ift.onlinelibrary.wiley.com/doi/10.1111/1541-4337.13250 by CochraneArgentina, Wiley Online Library on [13/10/2023]. See the Terms and Conditions (https://onlinelibrary.wiley.com/terms-and-conditions) on Wiley Online Library for rules of use; OA articles are governed by the applicable Creative Commons License

Qian, J., Yan, L., Ying, K., Luo, J., Zhuang, H., Yan, W., Zhang, J., & Zhao, Y. (2022). Plasma-activated water: A novel frozen meat thawing media for reducing microbial contamination on chicken and improving the characteristics of protein. *Food Chem*, *375*, 131661. https://doi.org/10.1016/j.foodchem.2021.131661

Rao, N. R. H., Chu, X., Hadinoto, K., Angelina, Zhou, R., Zhang, T., Soltani, B., Bailey, C. G, Trujillo, F. J., Leslie, G. L., Prescott, S. W., Cullen, P. J., & Henderson, R. K. (2023). Algal cell inactivation and damage via cold plasma-activated bubbles: Mechanistic insights and process benefits. *Chemical Engineering Journal*, *454*, 140304. https://doi.org/10.1016/j.cej.2022.140304

Rathore, V., & Nema, S. K. (2022). A comparative study of dielectric barrier discharge plasma device and plasma jet to generate plasma activated water and post-discharge trapping of reactive species. *Physics of Plasmas*, *29*(3), 033510. https://doi.org/10.1063/5.0078823

Rivero, W. C., Wang, Q., & Salvi, D. (2022). Impact of plasma-activated water washing on the microbial inactivation, color, and electrolyte leakage of alfalfa sprouts, broccoli sprouts, and clover sprouts. *Innovative Food Science & Emerging Technologies*, *81*, 103123. https://doi.org/10.1016/j.ifset.2022.103123

Roobab, U., Chacha, J. S., Abida, A., Rashid, S., Madni, G. M., Lorenzo, J. M., Zeng, X.-A., & Aadil, R. M. (2022). Emerging trends for nonthermal decontamination of raw and processed meat: Ozonation, high-hydrostatic pressure and cold plasma. *Foods*, *11*(15), 2173. https://doi.org/10.3390/foods11152173

Rosario, D. K. A., Rodrigues, B. L., Bernardes, P. C., & Conte-Junior, C. A. (2021). Principles and applications of non-thermal technologies and alternative chemical compounds in meat and fish. *Critical Reviews in Food Science and Nutrition*, *61*(7), 1163–1183. https://doi.org/10.1080/10408398.2020.1754755

Rothwell, J. G., Alam, D., Carter, D. A., Soltani, B., Mcconchie, R., Zhou, R., Cullen, P. J., & Mai-Prochnow, A. (2022). The antimicrobial efficacy of plasma-activated water against Listeria and E. coli is modulated by reactor design and water composition. *Journal of Applied Microbiology*, *132*(4), 2490–2500. https://doi.org/10.1111/jam.15429

Royintarat, T., Choi, E. H., Boonyawan, D., Seesuriyachan, P., & Wattanutchariya, W. (2020). Chemical-free and synergistic interaction of ultrasound combined with plasma-activated water (PAW) to enhance microbial inactivation in chicken meat and skin. *Scientific Reports*, *10*(1), 1559. https://doi.org/10.1038/s41598-020-58199-w

Royintarat, T., Seesuriyachan, P., Boonyawan, D., Choi, E. H., & Wattanutchariya, W. (2019). Mechanism and optimization of non-thermal plasma-activated water for bacterial inactivation by underwater plasma jet and delivery of reactive species underwater by cylindrical DBD plasma. *Current Applied Physics*, *19*(9), 1006–1014. https://doi.org/10.1016/j.cap.2019.05.020

Sampaio, A. D. G., Chiappim, W., Milhan, N. V. M., Botan Neto, B., Pessoa, R., & Koga-Ito, C. Y. (2022). Effect of the pH on the antibacterial potential and cytotoxicity of different plasma-activated liquids. *International Journal of Molecular Sciences*, *23*(22), 13893. https://doi.org/10.3390/ijms232213893

Schmidt, M., Hahn, V., Altrock, B., Gerling, T., Gerber, I. C., Weltmann, K.-D., & Von Woedtke, T. (2019). Plasma-activation of larger liquid volumes by an inductively-limited discharge for antimicrobial purposes. *Applied Sciences*, *9*(10), 2150. https://doi.org/10.3390/app9102150

Shaw, P., Kumar, N., Kwak, H. S., Park, J. H., Uhm, H. S., Bogaerts, A., Choi, E. H., & Attri, P. (2018). Bacterial inactivation by plasma treated water enhanced by reactive nitrogen species. *Scientific Reports*, *8*(1), 11268. https://doi.org/10.1038/s41598-018-29549-6

Shen, J., Tian, Y., Li, Y., Ma, R., Zhang, Q., Zhang, J., & Fang, J. (2016). Bactericidal effects against *S. aureus* and physicochemical properties of plasma activated water stored at different temperatures. *Scientific Reports*, *6*(1), 28505. https://doi.org/10.1038/srep28505

Shrestha, R., Pradhan, S. P., Guragain, R. P., Subedi, D. P., & Pandey, B. P. (2020). Investigating the effects of atmospheric pressure air DBD plasma on physio-chemical and microbial parameters of groundwater. *OALib*, *07*(03), 1–13. https://doi.org/10.4236/oalib.1106144

Simon, S., Salgado, B., Hasan, M. I., Sivertsvik, M., Fernández, E. N., & Walsh, J. L. (2021). Influence of potable water origin on the physicochemical and antimicrobial properties of plasma activated water. *Plasma Chemistry and Plasma Processing*, *42*(2), 377–393. https://doi.org/10.1007/s11090-021-10221-3

Šimončicová, J., Kryštofová, S., Medvecká, V., Ďurišová, K., & Kaliňáková, B. (2019). Technical applications of plasma treatments: Current state and perspectives. *Applied Microbiology and Biotechnology*, *103*(13), 5117–5129. https://doi.org/10.1007/s00253-019-09877-x

Sommers, B. S., & Foster, J. E. (2014). Plasma formation in underwater gas bubbles. *Plasma Sources Science and Technology*, *23*(1), 015020. https://doi.org/10.1088/0963-0252/23/1/015020

Su, X., Tian, Y., Zhou, H., Li, Y., Zhang, Z., Jiang, B., Yang, B., Zhang, J., & Fang, J. (2018). Inactivation efficacy of nonthermal plasma-activated solutions against Newcastle disease virus. *Applied and Environmental Microbiology*, *84*(9), e02836-17. https://doi.org/10.1128/AEM.02836-17

Subramanian, P. S. G., Ananthanarasimhan, J., Leelesh, P., Rao, H., Shivapuji, A. M., Girard-Lauriault, P.-L., & Rao, L. (2021). Plasma-activated water from DBD as a source of nitrogen for agriculture: Specific energy and stability studies. *Journal of Applied Physics*, *129*(9), 093303. https://doi.org/10.1063/5.0039253

Sysolyatina, E. V., Lavrikova, A. Y., Loleyt, R. A., Vasilieva, E. V., Abdulkadieva, M. A., Ermolaeva, S. A., & Sofronov, A. V. (2020). Bidirectional mass transfer-based generation of plasma-activated water mist with antibacterial properties. *Plasma Processes and Polymers*, *17*(10). https://doi.org/10.1002/ppap.202000058

Tabares, F. L., & Junkar, I. (2021). Cold plasma systems and their application in surface treatments for medicine. *Molecules*, *26*(7), 1903. https://doi.org/10.3390/molecules26071903

Tabu, B., Akers, K., Yu, P., Baghirzade, M., Brack, E., Drew, C., Mack, J. H., Wong, H.-W., & Trelles, J. P. (2022). Nonthermal atmospheric plasma reactors for hydrogen production from low-density polyethylene. *International Journal of Hydrogen Energy*, *47*(94), 39743–39757. https://doi.org/10.1016/j.ijhydene.2022.09.161

Tachibana, K., & Nakamura, T. (2019). Comparative study of discharge schemes for production rates and ratios of reactive oxygen and nitrogen species in plasma activated water. *Journal of Physics D: Applied Physics*, *52*(38), 385202. https://doi.org/10.1088/1361-6463/ab2529

Tsoukou, E., Bourke, P., & Boehm, D. (2020). Temperature stability and effectiveness of plasma-activated liquids over an 18 months period. *Water*, *12*(11), 3021. https://doi.org/10.3390/w12113021

Wang, J., Han, R., Liao, X., & Ding, T. (2021). Application of plasma-activated water (PAW) for mitigating methicillin-resistant

15414337, 0, Downloaded from https://ift.onlinelibrary.wiley.com/doi/10.1111/1541-4337.13250 by CochraneArgentina, Wiley Online Library on [13/10/2023]. See the Terms and Conditions (https://onlinelibrary.wiley.com/terms-and-conditions) on Wiley Online Library for rules of use; OA articles are governed by the applicable Creative Commons License

Staphylococcus aureus (MRSA) on cooked chicken surface. *LWT*, *137*, 110465. https://doi.org/10.1016/j.lwt.2020.110465

Wang, Q., & Salvi, D. (2021). Evaluation of plasma-activated water (PAW) as a novel disinfectant: Effectiveness on *Escherichia coli* and *Listeria innocua*, physicochemical properties, and storage stability. *LWT*, *149*, 111847. https://doi.org/10.1016/j.lwt.2021.111847

Wartel, M., Faubert, F., Dirlau, I. D., Rudz, S., Pellerin, N., Astanei, D., Burlica, R., Hnatiuc, B., & Pellerin, S. (2021). Analysis of plasma activated water by gliding arc at atmospheric pressure: Effect of the chemical composition of water on the activation. *Journal of Applied Physics*, *129*(23), 233301. https://doi.org/10.1063/5.0040035

Xia, B., Vyas, H. K. N., Zhou, R., Zhang, T., Hong, J., Rothwell, J. G., Rice, S. A., Carter, D., Ostrikov, K. K., Cullen, P. J., & Mai-Prochnow, A. (2023). The importance of superoxide anion for *Escherichia coli* biofilm removal using plasma-activated water. *Journal of Environmental Chemical Engineering*, *11*(3), 109977. https://doi.org/10.1016/j.jece.2023.109977

Xiang, Q., Fan, L., Li, Y., Dong, S., Li, K., & Bai, Y. (2022). A review on recent advances in plasma-activated water for food safety: Current applications and future trends. *Critical Reviews in Food Science and Nutrition*, *62*(8), 2250–2268. https://doi.org/10.1080/10408398.2020.1852173

Xiang, Q., Kang, C., Niu, L., Zhao, D., Li, K., & Bai, Y. (2018). Antibacterial activity and a membrane damage mechanism of plasma-activated water against *Pseudomonas deceptionensis* CM2. *LWT*, *96*, 395–401. https://doi.org/10.1016/j.lwt.2018.05.059

Xiang, Q., Kang, C., Zhao, D., Niu, L., Liu, X., & Bai, Y. (2019). Influence of organic matters on the inactivation efficacy of plasma-activated water against *E. coli* O157:H7 and *S. aureus*. *Food Control*, *99*, 28–33. https://doi.org/10.1016/j.foodcont.2018.12.019

Xiang, Q., Wang, W., Zhao, D., Niu, L., Li, K., & Bai, Y. (2019). Synergistic inactivation of *Escherichia coli* O157:H7 by plasma-activated water and mild heat. *Food Control*, *106*, 106741. https://doi.org/10.1016/j.foodcont.2019.106741

Xu, H., Liu, C., & Huang, Q. (2023). Enhance the inactivation of fungi by the sequential use of cold atmospheric plasma and plasma-activated water: Synergistic effect and mechanism study. *Chemical Engineering Journal*, *452*, 139596. https://doi.org/10.1016/j.cej.2022.139596

Yong, H. I., Park, J., Kim, H.-J., Jung, S., Park, S., Lee, H. J., Choe, W., & Jo, C. (2018). An innovative curing process with plasma-treated water for production of loin ham and for its quality and safety. *Plasma Processes and Polymers*, *15*(2), 1700050. https://doi.org/10.1002/ppap.201700050

Yoon, S.-Y., Jeon, H., Yi, C., Park, S., Ryu, S., & Kim, S. B. (2018). Mutual interaction between plasma characteristics and liquid properties in AC-driven pin-to-liquid discharge. *Scientific Reports*, *8*(1), 12037. https://doi.org/10.1038/s41598-018-30540-4

Zhang, Q., Ma, R., Tian, Y., Su, B., Wang, K., Yu, S., Zhang, J., & Fang, J. (2016). Sterilization efficiency of a novel electrochemical disinfectant against *Staphylococcus aureus*. *Environmental Science & Technology*, *50*(6), 3184–3192. https://doi.org/10.1021/acs.est.5b05108

Zhao, Y.-M., Ojha, S., Burgess, C. M., Sun, D.-W., & Tiwari, B. K. (2020a). Inactivation efficacy and mechanisms of plasma activated water on bacteria in planktonic state. *Journal of Applied Microbiology*, *129*(5), 1248–1260. https://doi.org/10.1111/jam.14677

Zhao, Y. M., Ojha, S., Burgess, C. M., Sun, D. W., & Tiwari, B. K. (2020b). Influence of various fish constituents on inactivation efficacy of plasma-activated water. *International Journal of Food Science & Technology*, *55*(6), 2630–2641. https://doi.org/10.1111/ijfs.14516

Zhao, Y., Zhao, Z., Chen, R., Tian, E., Liu, D., Niu, J., Wang, W., Qi, Z., Xia, Y., & Song, Y. (2020c). Plasma-Activated water treatment of fresh beef: Bacterial inactivation and effects on quality attributes. *IEEE Transactions on Radiation and Plasma Medical Sciences*, *4*(1), 113–120. https://doi.org/10.1109/trpms.2018.2883789

Zhao, Y.-M., Oliveira, M., Burgess, C. M., Cropotova, J., Rustad, T., Sun, D.-W., & Tiwari, B. K. (2021). Combined effects of ultrasound, plasma-activated water, and peracetic acid on decontamination of mackerel fillets. *LWT*, *150*, 111957. https://doi.org/10.1016/j.lwt.2021.111957

Zhou, R., Zhang, T., Zhou, R., Mai-Prochnow, A., Ponraj, S. B., Fang, Z., Masood, H., Kananagh, J., Mcclure, D., Alam, D., Ostrikov, K. K., & Cullen, P. J. (2021). Underwater microplasma bubbles for efficient and simultaneous degradation of mixed dye pollutants. *Science of The Total Environment*, *750*, 142295. https://doi.org/10.1016/j.scitotenv.2020.142295

Zhou, R., Zhou, R., Prasad, K., Fang, Z., Speight, R., Bazaka, K., & Ostrikov, K. K. (2018). Cold atmospheric plasma activated water as a prospective disinfectant: The crucial role of peroxynitrite. *Green Chemistry*, *20*(23), 5276–5284. https://doi.org/10.1039/c8gc02800a

Zhou, R., Zhou, R., Wang, P., Xian, Y., Mai-Prochnow, A., Lu, X., Cullen, P. J., Ostrikov, K. K., & Bazaka, K. (2020). Plasma-activated water: Generation, origin of reactive species and biological applications. *Journal of Physics D: Applied Physics*, *53*(30), 303001. https://doi.org/10.1088/1361-6463/ab81cf

Zhu, W., Tan, G., Han, M., Bu, Y., Li, X., & Li, J. (2023). Evaluating the effects of plasma-activated slightly acidic electrolyzed water on bacterial inactivation and quality attributes of Atlantic salmon fillets. *Innovative Food Science & Emerging Technologies*, *84*, 103286. https://doi.org/10.1016/j.ifset.2023.103286

How to cite this article: Hadinoto, K., Niemira, B. A., & Trujillo, F. J. (2023). A review on plasma-activated water and its application in the meat industry. *Comprehensive Reviews in Food Science and Food Safety*, 1–27. https://doi.org/10.1111/1541-4337.13250

15414337, 0, Downloaded from https://ift.onlinelibrary.wiley.com/doi/10.1111/1541-4337.13250 by CochraneArgentina, Wiley Online Library on [13/10/2023]. See the Terms and Conditions (https://onlinelibrary.wiley.com/terms-and-conditions) on Wiley Online Library for rules of use; OA articles are governed by the applicable Creative Commons License